Lawrence Berkeley National Laboratory
LBL Publications

Title
Treatment of Pionic Modes at the Nuclear Surface for Transport Descriptions

Permalink
https://escholarship.org/uc/item/9hm4b86b

Authors
Helgesson, J.
Randrup, Jorgen

Publication Date
1995-08-21

eScholarship.org Powered by the California Digital Library
University of California

LBL-37623
UC-413
Preprint

Lawrence Berkeley Laboratory
UNIVERSITY OF CALIFORNIA

Submitted to Nuclear Physics A

Treatment of Pionic Modes at the Nuclear Surface for Transport Descriptions

J. Helgesson and J. Randrup

August 1995

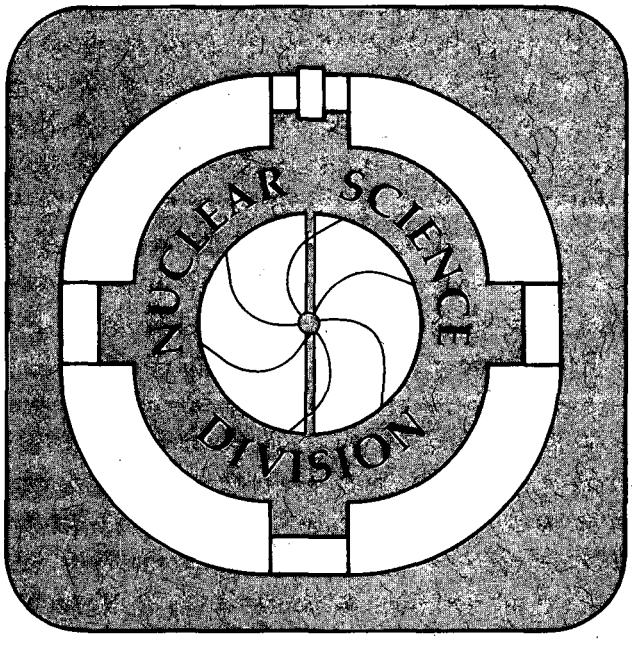

REFERENCE COPY
Does Not
Circulate
LBL-37623
Copy 1
Bldg. 50 Library.

Prepared for the U.S. Department of Energy under Contract Number DE-AC03-76SF00098

DISCLAIMER

This document was prepared as an account of work sponsored by the United States Government. While this document is believed to contain correct information, neither the United States Government nor any agency thereof, nor the Regents of the University of California, nor any of their employees, makes any warranty, express or implied, or assumes any legal responsibility for the accuracy, completeness, or usefulness of any information, apparatus, product, or process disclosed, or represents that its use would not infringe privately owned rights. Reference herein to any specific commercial product, process, or service by its trade name, trademark, manufacturer, or otherwise, does not necessarily constitute or imply its endorsement, recommendation, or favoring by the United States Government or any agency thereof, or the Regents of the University of California. The views and opinions of authors expressed herein do not necessarily state or reflect those of the United States Government or any agency thereof or the Regents of the University of California.

Nuclear Physics A LBL-37623

Treatment of Pionic Modes at the Nuclear Surface for Transport Descriptions*

Johan Helgesson and Jørgen Randrup

Nuclear Science Division, Lawrence Berkeley Laboratory
University of California, Berkeley, California 94720

August 21, 1995

Abstract:

Dispersion relations and amplitudes of collective pionic modes are derived in a $\pi + NN^{-1} + \Delta N^{-1}$ model for use in transport descriptions by means of a local density approximation. It is discussed how pionic modes can be converted to real particles when penetrating the nuclear surface and how earlier treatments can be improved. When the surface is stationary only free pions emerge. The time-dependent situation is also addressed, as is the conversion of non-physical (*i.e.* unperturbed ΔN^{-1}) modes to real particles when the nuclear density vanishes. A simplified one-dimensional scenario is used to investigate the reflection and transmission of pionic modes at the nuclear surface. It is found that reflection of pionic modes is rather unlikely, but the process can be incorporated into transport descriptions by the use of approximate local transmission coefficients.

*This work was supported by the Swedish Natural Science Research Council and by the Director, Office of Energy Research, Office of High Energy and Nuclear Physics, Nuclear Physics Division of the U.S. Department of Energy under Contract No. DE-AC03-76SF00098.

1 Introduction

In collisions between two heavy nuclei at bombarding energies from a few hundred MeV up to several GeV per nucleon, hadronic matter at high density and temperature is formed. In such collisions a large number of energetic particles are produced and may be used as probes of the hot and dense phase of the reaction [1, 2, 3].

Microscopic transport models, such as BUU and QMD [2, 3, 4, 5] have been fairly successful in describing particle production in heavy-ion reactions. In these transport models, the nucleons propagate in an effective one-body field while subject to direct two-body collisions. Sufficiently energetic nucleon-nucleon collisions may agitate one or both of the colliding nucleons to a nucleon resonance, especially $\Delta(1232)$, $N^*(1440)$, and $N^*(1535)$. Such resonances propagate in their own mean field and may collide with nucleons or other nucleon resonances as well. Furthermore, the nucleon resonances may decay by meson emission and these decay processes constitute the main mechanisms for the production of energetic mesons [3].

The transport descriptions normally employ the vacuum properties of the resonances and mesons, *i.e.* the needed cross sections, decay widths, and dispersion relations are taken according to their values in vacuum [4]. However, in infinite nuclear matter, a system of interacting π mesons, nucleons, and Δ isobars will couple to form spin-isospin modes. Some of these modes are non-collective in their character, dominated by a single baryon-hole excitation, while other modes are collective and correspond to meson-like states (quasimesons). The non-collective spin-isospin modes correspond to those already included in transport simulations by promoting a nucleon from below to above the Fermi surface. The collective spin-isospin modes can effectively be regarded as particles of mesonic character (quasimesons), which by means of a local density and temperature approximation can be incorporated into the transport descriptions.

Some in-medium modifications have already been employed in calculations of heavy-ion collisions, both qualitatively [6] and by transport simulations [7, 8, 9]. A more elaborate $\pi + NN^{-1} + \Delta N^{-1}$ model was employed in ref. [10] to derive several quantities useful for implementation of in-medium properties in transport descriptions. While it is straightforward to apply the local density approximation in the interior regions of the nuclear system, there are conceptual problems of how to proceed at the nuclear surface where the density approaches zero and the quasimesons convert to real physical particles. The problem is that while in a real system no hole states exist in vacuum, a collective (ΔN^{-1}-like) mode can in a stationary infinite system exist for an arbitrary small (but finite) density. This is because the particles in the stationary system have infinite time to explore the entire system and form collective modes also at extremely low densities.

In this paper we will therefore discuss how a proper conversion from quasimesons to real particles at the surface can be performed. Earlier works [8, 9] have treated this conversion by various approximations (see further the discussion in section 4). In this work we will present a somewhat different approach, based on ref. [10], and discuss how the approximations in the earlier works can be improved upon.

The present paper constitutes a qualitative investigation of treatment of pionic

modes at a nuclear surface in transport simulations. To make the presentation simple and transparent we will therefore restrict ourselves to some special cases of the more complete investigation in ref. [10]. We will only consider the collective modes in the spin-longitudinal channel (pion like), since this is the dominant channel at the energies we have in mind in this paper. Collective modes in the spin-transverse channel (ρ meson like) can be treated completely analogously. Furthermore we will consider the zero-temperature case, and the Δ width will not be included in the calculation of the dispersion relations (denoted as the reference case in ref. [10]).

The justification for considering only $T = 0$ in this paper is that there is not a strong dependence on the dispersion relations of the collective modes for moderately large temperatures, especially not at low densities at the surface. Also, the temperature is not expected to be very high at the surface. However we want to emphasize that there is no principal difficulty associated with incorporating $T > 0$ in the treatment.

The motivation for omitting the Δ width, in the calculation of the dispersion relations, is somewhat more involved. Including the Δ width self-consistently in the calculation of the spin-isospin modes encompasses decay processes like

$$\tilde{\pi}_j \rightarrow \Delta N^{-1} \rightarrow (N + \tilde{\pi}_k) N^{-1} \ .$$

However, since such processes are already explicitly contained in the transport simulation by processes like

$$\tilde{\pi}_j + N \rightarrow \Delta \rightarrow N + \tilde{\pi}_k \ ,$$

it does not seem to be correct to include the entire self-consistent Δ width when calculating the collective modes to be used in the transport description. Instead it seems more correct to use the results obtained with the Δ width omitted, both for the energies of the modes and for the partial Δ widths to be used in the decays $\Delta \rightarrow N + \tilde{\pi}_j$.

However one should note that by omitting the Δ width in the dispersion relations one also fails to take into account the fact that the pionic modes have a Breit-Wigner like energy distribution, analogous with the Δ. The width and center of this distribution are determined by the the self-consistent Δ width and depends on the particular pionic mode and its momentum. The center of the distribution approximately corresponds to the energy found when the Δ width is omitted [10].

In section 2 we will give a brief presentation of the model. The dispersion relations and amplitudes of the spin-isospin modes obtained in infinite nuclear matter, are presented and discussed in section 3. Section 4 is devoted to a discussion of the pionic modes at a nuclear surface and the implications for transport descriptions, while our results are summarized in section 5. In addition we present in appendix A a discussion of reflection and transmission properties at the nuclear surface, and in appendix B some technical details for the RPA equations.

2 The model

The model presented in this section is treated and motivated in detail in ref. [10]. For convenience we here present a brief recapitulation of the essential points. Furthermore, the presentation in this section only treats the spin-longitudinal channel for the special case when $T = 0$ and the Δ width is omitted in the calculation of the spin-isospin modes.

2.1 Spin-isospin modes in an infinite system

We consider a system of interacting nucleons (N), delta isobars (Δ) and pi mesons (π). In order to investigate the in-medium properties of the interacting particles, we employ a cubic box with side length L; the calculated properties are not sensitive to the actual size, so we need not take the limit $L \to \infty$ explicitly.

The in-medium properties are obtained by using the Green's function technique, starting from non-interacting hadrons. The non-interacting Hamiltonian can be written

$$H_0 = \sum_k e_k \hat{b}_k^\dagger \hat{b}_k + \sum_l \hbar\omega_\pi(\boldsymbol{q}_l)\hat{\pi}_l^\dagger \hat{\pi}_l \ . \tag{1}$$

Here the index $k = (\boldsymbol{p}_k;\, s_k, m_{s_k};\, t_k, m_{t_k})$ represents the baryon momentum, spin, and isospin. The spin and isospin quantum numbers, s_k and t_k, take the values $\frac{1}{2}$ and $\frac{3}{2}$ for N and Δ, respectively. The energy of baryon k moving in a (spatially constant) potential is denoted e_k. The baryon creation and annihilation operators, $\hat{b}_k^\dagger$ and $\hat{b}_k$, are normalized such that they satisfy the usual anti-commutation relation,

$$\{\hat{b}_k^\dagger,\, \hat{b}_{k'}\} = \delta_{k,k'} \ . \tag{2}$$

In the pion part of H_0, the index l represents the pion momentum and isospin, $l = (\boldsymbol{p}_l, \lambda_l = 0, \pm 1)$. The meson energy is given by $\hbar\omega_\pi = [m_\pi^2 + \boldsymbol{q}^2]^{1/2}$ and the creation and annihilation operators of the pion are normalized such that they satisfy the usual commutation relation,

$$[\hat{\pi}_l^\dagger,\, \hat{\pi}_{l'}] = \delta_{l,l'} \ . \tag{3}$$

Note that the Δ isobar described by H_0 has no decay width, $\Gamma_\Delta = 0$. When the interactions are turned on, the Δ width will emerge and it will then automatically include also the free width.

2.1.1 Basic interactions

At the $N\pi N$ and $N\pi\Delta$ vertices we will use effective p-wave interactions, $V_{N\pi N}$ and $V_{N\pi\Delta}$, which in the momentum representation can be written as [10, 11]

$$V_{N\pi N} = ic\frac{(\hbar c)^{\frac{1}{2}}}{L^3}\left[\frac{2m_N c^2}{m_N c^2 + \sqrt{s}}\right]^{\frac{1}{2}} \frac{f_{NN}^\pi}{m_\pi c^2}\, F_\pi(q)\, (\boldsymbol{\sigma}\cdot\boldsymbol{q}_{cm})\ \vec{\tau}\cdot\overleftarrow{\phi}_\pi\,(\boldsymbol{q}) \tag{4}$$

$$V_{N\pi\Delta} = ic\frac{(\hbar c)^{\frac{1}{2}}}{L^3}\left[\frac{2m_\Delta c^2}{m_\Delta c^2 + \sqrt{s}}\right]^{\frac{1}{2}} \frac{f_{N\Delta}^\pi}{m_\pi c^2}\, F_\pi(q)\, (\boldsymbol{S}^+\cdot\boldsymbol{q}_{cm})\ \vec{T}^+\cdot\overleftarrow{\phi}_\pi\,(\boldsymbol{q}) + \text{h.c.} \tag{5}$$

In these expressions, $\sqrt{s}$ is the center-of-mass energy in the $N\pi$ system and $\boldsymbol{q}_{cm}$ is the pion momentum in the $N\pi$ center-of-mass system, which in the non-relativistic limit is given by

$$\boldsymbol{q}_{cm} \approx \frac{m_N c^2}{m_N c^2 + \hbar\omega}\, \boldsymbol{q} - \frac{\hbar\omega}{m_N c^2 + \hbar\omega}\, \boldsymbol{p}_N \ , \tag{6}$$

where $\hbar\omega$ and $\boldsymbol{q}$ is the pion energy and momentum, and $\boldsymbol{p}_N$ is the nucleon momentum in an arbitrary frame. The Pauli spin and isospin matrices are denoted $\boldsymbol{\sigma}$ and $\vec{\tau}$, and $\boldsymbol{S}^+$ and $\vec{T}^+$ are spin and isospin $\frac{1}{2}$ to $\frac{3}{2}$ transition operators normalized such that $< \frac{3}{2}, \frac{3}{2} | S^+_{+1} | \frac{1}{2}, \frac{1}{2} >= 1$.[1] The momentum representation of the pion field is taken as

$$\phi^\pi_\lambda(\boldsymbol{q}) = \frac{L^{3/2}\hbar c}{\sqrt{2\hbar\omega_\pi(\boldsymbol{q})}} \left[\hat{\pi}_\lambda(\boldsymbol{q}) + (-1)^\lambda \hat{\pi}^\dagger_{-\lambda}(-\boldsymbol{q}) \right] \ . \tag{7}$$

The interactions contain a monopole form factor,

$$F_\pi(q) = \frac{\Lambda_\pi^2 - (m_\pi c^2)^2}{\Lambda_\pi^2 - (cq)^2} \ , \tag{8}$$

and the coupling constants are determined at $(cq)^2 = (\hbar\omega)^2 - (c\,\boldsymbol{q})^2 = (m_\pi c^2)^2$ and $\sqrt{s} = m_N c^2$ or $\sqrt{s} = m_\Delta c^2$.

In addition we will also include effective short-range interactions at nucleon-hole vertices, again written in momentum space,

$$V_{NN^{-1},NN^{-1}} = \left(\frac{\hbar c}{L}\right)^3 g'_{NN} \left(\frac{f^\pi_{NN}}{m_\pi}\right)^2 |F_g(q)|^2 \ (\boldsymbol{\sigma}_1 \cdot \boldsymbol{\sigma}_2)(\vec{\tau}_1 \cdot \vec{\tau}_2) \ , \tag{9}$$

and the corresponding interactions obtained when one (or two) of the nucleons is replaced by a Δ. The strength of the short-range interactions is determined by the correlation parameters g'_{NN}, $g'_{N\Delta}$, and $g'_{\Delta\Delta}$.

2.2 RPA approximation

We want to calculate a spin-isospin mode Green's function within the RPA approximation, symbolically

$$G^{\mathrm{RPA}}(\alpha,\beta;\omega) = G_0(\alpha,\beta;\omega) + \sum_{\gamma,\kappa} G_0(\alpha,\gamma;\omega)\ \mathcal{V}(\gamma,\kappa;\omega)\ G^{\mathrm{RPA}}(\kappa,\beta;\omega) \ . \tag{10}$$

The spin-isospin modes, here represented by the Green's function G^{RPA}, will in this approximation be obtained as an infinite iteration of (non-interacting) pion, nucleon-hole, and Δ-hole states, represented by the diagonal Green's function G_0, coupled with the interactions specified in eqs. (4–9) which here are summarized by the symbolic interaction $\mathcal{V}$.

[1] For clarity, we generally employ bold-face characters to denote quantities with vector and tensor properties under ordinary spatial rotations, while arrows are employed to indicate the transformation properties under rotations in isospace.

In nuclear collisions at beam energies up to about one GeV per nucleon, which is the domain of application that we have in mind, only relatively few mesons and isobars are produced and so the associated quantum-statistical effects may be ignored. Accordingly, we assume $n_\Delta \ll 1$, and $n_\pi \ll 1$.

A set of RPA equations, equivalent to eq. (10) were derived in ref. [10]. From these equations eigenvectors and eigenenergies are obtained for the different spin-isospin modes. The eigenvectors will yield the amplitudes of the different components (π, NN^{-1}, ΔN^{-1}) forming the particular spin-isospin mode with the given eigenenergy. These RPA amplitudes contain important information about the nature of the different spin-isospin modes. The spin-isospin modes (or excited RPA states), $|\Psi_\nu>$, are created by an operator $Q^\dagger_\nu$,

$$Q^\dagger_\nu(\boldsymbol{q},\lambda) = \sum_{jk} X^\nu_{jk}(\boldsymbol{q},\lambda)\hat{b}^\dagger_j\hat{b}_k + \sum_k Z^\nu_k(\boldsymbol{q},\lambda)\,\hat{\pi}^\dagger_k - \sum_k W^\nu_k(\boldsymbol{q},\lambda)\,\hat{\pi}_k \ . \tag{11}$$

The quantity $X^\nu_{jk}(\boldsymbol{q},\lambda)$ is here the amplitude of the baryon-hole (NN^{-1} or ΔN^{-1}) component of the spin-isospin mode $|\Psi_\nu>$ at momentum $\boldsymbol{q}$ and isospin λ, while $Z^\nu_k(\boldsymbol{q},\lambda)$ and $W^\nu_k(\boldsymbol{q},\lambda)$, in the same way, are the amplitudes of the pionic component. The summation over baryon and meson states in eq. (11) is restricted by taking $X_{jk} \propto \delta_{\boldsymbol{p}_j,\boldsymbol{p}_k+\boldsymbol{q}}$, $Z_k \propto \delta_{\boldsymbol{p}_k,\boldsymbol{q}}\delta_{\lambda_k,\lambda}$, and $W_k \propto \delta_{\boldsymbol{p}_k,-\boldsymbol{q}}\delta_{\lambda_k,-\lambda}$.

The RPA equations are obtained from the relation

$$< [\delta Q,[H,Q^\dagger]] >= \hbar\omega < [\delta Q, Q^\dagger] > \ , \tag{12}$$

with $\delta Q = \hat{b}^\dagger_k\hat{b}_j$, $\hat{\pi}_\tau$, or $\hat{\pi}^\dagger_\tau$, and where the brackets $< \cdot >$ denote the expectation value in the interacting ground state. It can be shown that the set of RPA solutions constitutes an orthonormal set. For convenience the solutions of the RPA equations of ref. [10], are recapitulated in appendix B.

2.2.1 The total Δ width

The Δ self energy Σ_Δ is calculated according to the diagrams in fig. 1, by taking into account all the diagrams corresponding to the Δ decaying into a spin-isospin mode and a nucleon, which then again form a Δ. In the spin-longitudinal channel we obtain (ref. [10])

$$\Gamma^l_\Delta(E_\Delta,\boldsymbol{p}_\Delta) = \mathrm{Im}\,\frac{2}{3}\left(\frac{\hbar c}{L}\right)^3 \sum_{\boldsymbol{q}} [\theta(\mathcal{E}) - n(\boldsymbol{p}_\Delta - \boldsymbol{q})]\,\bar{M}(\Delta N, N\Delta) \ . \tag{13}$$

where the energy available for the spin-isospin mode is given by

$$\mathcal{E} = E_\Delta - \epsilon_N(\boldsymbol{p}_\Delta - \boldsymbol{q}) \ , \tag{14}$$

and $\bar{M}(34,12)$ can be expressed as

$$\bar{M}(34,12) = \sum_{\omega_\nu>0}\left\{\frac{h(31;\nu)h(24;\nu)}{\hbar\omega - \hbar\omega_\nu + i\eta} - \frac{h(31;\nu)h(24;\nu)}{\hbar\omega + \hbar\omega_\nu - i\eta}\right\} + \frac{f^\pi_{31}f^\pi_{24}}{(m_\pi c^2)^2}F_g^2 g'_{34,12} \ . \tag{15}$$

The factor $h(jk,\nu)$ is obtained from the interactions at the vertex consisting of baryons j and k, and the spin-isospin mode ν. The interactions to be used depend on the non-interacting states that the mode consists of and must therefore be multiplied by the amplitude of the corresponding state,

$$h(jk,\nu)\vartheta^l(jk) = \frac{V_{j\pi k}}{\sqrt{2\hbar\omega_\pi}}\left[Z(\nu)+W(\nu)\right] + \sum_{mn} V_{jk,mn}\, X_{mn}(\nu)\ , \tag{16}$$

where $\vartheta^l(jk)$ is a short hand notation for the spin-isospin matrix elements in the spin-longitudinal channel, $V_{j\pi k}$ is defined in (4) and (5), $V_{jk,mn}$ is defined in (9), and the amplitudes X^l_{mn}, Z^l, W^l are defined in eq. (11). The explicit expression for $h(jk,\nu)$ is somewhat lengthy and has therefore also been relegated to appendix B.

2.2.2 Specific Δ channels

The total Δ width gives the transition probability per unit time for the Δ resonance to decay to any of its decay channels. In a transport description one explicitly allows the Δ resonance to decay into specific final particles. Consequently, one needs not only the total Δ width (which is the sum of all decay channels) but also the partial widths governing the decay into specific RPA channels. These decay channels consist of a nucleon and one of the spin-isospin modes. Since we have access to all the amplitudes of a given spin-isospin mode on the different unperturbed states, it is possible to derive an expression for the partial contribution to Γ_Δ from the Δ decay to a specific mode ν. The right-hand side of fig. 1 shows a diagrammatic representation of such a process. The partial Δ width for a Δ decay to a nucleon and a spin-longitudinal mode ν becomes [10]

$$\begin{aligned}\tilde{\Gamma}^\nu_\Delta(E_\Delta,\boldsymbol{p}_\Delta) &= \int \frac{d^3p_N}{(2\pi)^3}\frac{d^3q}{(2\pi)^3}\,\Big|\frac{V_{\Delta\pi N}}{\sqrt{2\hbar\omega_\pi}}\cdot\left[Z(\nu)+W(\nu)\right] + \sum_{mn} V_{\Delta N,mn}\cdot X_{mn}(\nu)\Big|^2 \\ &\quad \times\bar{n}_N(\boldsymbol{p}_N)\,(2\pi)^3\delta(\boldsymbol{p}_\Delta-\boldsymbol{p}_N-\boldsymbol{q})2\pi\delta(E_\Delta-e_N-\hbar\omega) \\ &= \frac{1}{3}\int\frac{d^3q}{(2\pi)^3}\,|h(\Delta N,\omega_\nu)|^2\,\bar{n}_N(\boldsymbol{p}_\Delta-\boldsymbol{q})\,2\pi\delta(E_\Delta-e_N-\hbar\omega_\nu)\end{aligned} \tag{17}$$

where the factor, $\bar{n}_N = 1-n_N$, takes into account the Pauli blocking of the nucleon. Note that when this expression is to be used in transport models the factor $\bar{n}_N$ should be omitted since the Pauli blocking is treated explicitly in the transport description. The expression (17) is identical to the contribution from one of the ν terms in eq. (13).

3 Dispersion relations and amplitudes

From eq. (59) in appendix B we calculate the energies of the spin-isospin modes that are formed in the interacting system, *i.e.* their dispersion relations. Fig. 2 displays the dispersion relations at normal nuclear density, $\rho = \rho^0 = 0.153$ fm^{-3}. In fig. 2 a number of different modes in the spin-longitudinal (π-like) channel are apparent.

Some of those are non-collective NN^{-1} modes (solid curves), which have their energies within the regions

$$\begin{aligned} 0 \;\leq\; \hbar\omega \;\leq\; \frac{q^2}{2m_N^*} + \frac{qp_F}{m_N^*}\,, \qquad & q < 2p_F\,, \\ \frac{q^2}{2m_N^*} - \frac{qp_F}{m_N^*} \;\leq\; \hbar\omega \;\leq\; \frac{q^2}{2m_N^*} + \frac{qp_F}{m_N^*}\,, \qquad & q > 2p_F\,. \end{aligned} \tag{18}$$

Since we are presenting our results for a box normalization with a finite side length L, we obtain a discrete number of non-collective NN^{-1} modes. The total number of spin-isospin modes within the region (18) depends on L and tends towards a continuum in the limit $L \to \infty$. Similarly, a number of non-collective ΔN^{-1} states emerge in fig. 2 which, for a fixed $\boldsymbol{q}$, have their energies constrained to a band,

$$m_\Delta - m_N + \frac{q^2}{2m_\Delta} - \frac{qp_F}{m_\Delta} \;\leq\; \hbar\omega \;\leq\; m_\Delta - m_N + \frac{q^2}{2m_\Delta} + \frac{qp_F}{m_\Delta}\,. \tag{19}$$

The non-collective baryon-hole modes correspond in a transport description to propagation of uncoupled baryons (N or Δ). This was discussed and studied in detail in ref. [10] and will therefore not be further discussed in this paper.

In addition, two collective modes appear in fig. 2, represented by dot-dashed curves. The lower one starts at $\hbar\omega = m_\pi c^2$ at $q = 0$ and continues into the ΔN^{-1} region around $q \approx 360$ MeV/c. This mode will in the following be referred to as $\tilde{\pi}_1$. The upper collective mode starts slightly above $\hbar\omega \approx m_\Delta c^2 - m_N c^2$ at $q = 0$ and approaches $\hbar\omega_\pi = [(m_\pi c^2)^2 + (cq)^2]^{1/2}$ at large q. This mode is denoted $\tilde{\pi}_2$.

The incorporation of the two collective spin-isospin modes into transport equations is more involved. These modes can be regarded as separate particles of pionic character, $\tilde{\pi}_1$ and $\tilde{\pi}_2$, and treated in a manner analogous to the standard treatment of the pion. Since the pion is then fully included in the description, it should no longer be treated explicitly. The propagation of the two collective pionic modes is governed by the effective Hamiltonians

$$\begin{aligned} \tilde{H}_1(\boldsymbol{r},\boldsymbol{q}) \;&=\; \hbar\omega_1(\boldsymbol{q};\rho(\boldsymbol{r})) \;\equiv\; \hbar\tilde{\omega}_1\,, \\ \tilde{H}_2(\boldsymbol{r},\boldsymbol{q}) \;&=\; \hbar\omega_2(\boldsymbol{q};\rho(\boldsymbol{r})) \;\equiv\; \hbar\tilde{\omega}_2\,, \end{aligned} \tag{20}$$

where $\hbar\omega_1$ and $\hbar\omega_2$ are the energy-momentum relations for the lower and upper collective modes displayed in fig. 2 for $\rho = \rho^0$. Note that the spatial dependence of $\tilde{H}_1(\boldsymbol{r},\boldsymbol{q})$ is incorporated by representing $\rho(\boldsymbol{r})$ as a local quantity. To facilitate center-of-mass transformations we parametrize the dispersion relations of the pionic modes in the form

$$\hbar\tilde{\omega}(\boldsymbol{q};\rho) \approx \left\{[c\,q - c\,q_0(\rho)]^2 + m_0(\rho)^2c^4\right\}^{\frac{1}{2}} + U_0(\rho) \tag{21}$$

For convenience in the transport simulations, we have chosen to use relatively simple expressions for the parametrization, rather than to try to optimize the fit. In this way a quasipion moves like a relativistic particle with the group velocity determined by an effective momentum and energy

$$\frac{d\hbar\tilde{\omega}}{dq} = c\frac{c(q-q_0)}{\hbar\tilde{\omega} - U_0} = c\frac{cq^*}{\hbar\tilde{\omega}^*}\,. \tag{22}$$

The density-dependent parameters q_0, m_0 and U_0 are presented in fig. 3.

Furthermore, in the collision term of the standard transport description the process for the production and absorption of pions $\Delta \leftrightarrow N + \pi$, should be replaced by the two distinct processes

$$\Delta \leftrightarrow N + \tilde{\pi}_1 \quad \text{and} \quad \Delta \leftrightarrow N + \tilde{\pi}_2 \, . \tag{23}$$

The Δ decay is governed by the Δ decay width in the medium to these two specific channels, $\tilde{\Gamma}^j_\Delta$. These partial widths, should be employed in the same manner as the free width, *i.e.* they describe the probability for the Δ isobar to decay into a nucleon and a pion. The only difference is that several collective pionic modes are available in the final state. In fig. 4 we present total and partial Δ widths for a Δ with the momentum 300 MeV/c. The reverse processes in (23) are characterized by cross sections that were presented and discussed in ref. [10]. To obtain the partial Δ width from eq. (17) it is necessary to know the amplitudes Z, $\sum X_{\Delta N^{-1}}$ and $\sum X_{NN^{-1}}$. We therefore also present a parametrization of these quantities. On the lower pionic mode the pionic component dominates for small momenta, q, and the ΔN^{-1} component dominates at larger momenta. Therefore the sum of all individual ΔN^{-1} components will for small q increase with q. However, when the lower pionic mode enters the ΔN^{-1} region the collectivity disappears gradually, and the sum of all individual ΔN^{-1} components starts to decrease with q. Thus we employ the form

$$\sum X^{\tilde{\pi}_1}_{\Delta N^{-1}}(\boldsymbol{q};\rho) \approx f_\Delta(q, \vec{C}[X^{\tilde{\pi}_1}_{\Delta N^{-1}}]) \, , \tag{24}$$

$$\sum X^{\tilde{\pi}_1}_{NN^{-1}}(\boldsymbol{q};\rho) \approx f_N(q, \vec{C}[X^{\tilde{\pi}_1}_{NN^{-1}}]) \, , \tag{25}$$

with

$$f_{\substack{\Delta \\ N}}(q, \vec{C}) = \frac{\pm C_1^2 + C_2\, cq}{C_3^2 + (cq - C_4)^2} \, . \tag{26}$$

The density-dependent coefficients $\vec{C}$ are presented in fig. 5. On the upper pionic mode we instead parametrize the amplitudes as

$$\sum X^{\tilde{\pi}_2}_{\Delta N^{-1}}(\boldsymbol{q};\rho) \approx C'_N[X^{\tilde{\pi}_2}_{\Delta N^{-1}}]\sqrt{f_2(q, \vec{C}'[X^{\tilde{\pi}_2}_{\Delta N^{-1}}])} \tag{27}$$

$$\sum X^{\tilde{\pi}_2}_{NN^{-1}}(\boldsymbol{q};\rho) \approx C'_N[X^{\tilde{\pi}_2}_{NN^{-1}}]\sqrt{1 - f_2(q, \vec{C}'[X^{\tilde{\pi}_2}_{NN^{-1}}])} \, , \tag{28}$$

where

$$f_2(q, \vec{C}') = \left[1 + \exp\left(C'_0 + C'_1\, cq + C'_{-1}/cq\right)\right]^{-1} \, , \tag{29}$$

with the density-dependent coefficients $\vec{C}'$, displayed in fig. 6. The amplitudes Z of the pion component are obtained from the parametrization of the squared amplitudes, eqs. (30) and (31) below, as $Z = \sqrt{Z^2}$.

The total Δ decay width, has apart from the partial contributions $\tilde{\Gamma}^j_\Delta$, also the partial contributions $\Gamma^{NN^{-1}}_\Delta$ and $\Gamma^{\Delta N^{-1}}_\Delta$. The partial width $\Gamma^{NN^{-1}}_\Delta$ gives the probability for the Δ to decay into a nucleon and a NN^{-1} state. In a transport description, this implies that we initially have a Δ and after the decay process we have two nucleons above the Fermi surface and a hole left in the Fermi sea. But this is the same

process as if the Δ would collide with a nucleon below the Fermi surface to give two nucleons above the Fermi surface. This process is normally already included in the collision term in a standard transport description, and the probability for such a collision is given by the cross section for the process $\Delta + N \rightarrow N + N$. In a transport description it is therefore not correct to both include a Δ decay according to $\Gamma_\Delta^{NN^{-1}}$ and a collision term with $\Delta + N \rightarrow N + N$. Instead, the correct procedure should be to exclude $\Gamma_\Delta^{NN^{-1}}$ and modify the cross section $\sigma(\Delta + N \rightarrow N + N)$ to be the in-medium cross section. Calculations of such in-medium cross sections was discussed in ref. [10]. In the same way, $\Gamma_\Delta^{\Delta N^{-1}}$ should be excluded in a transport description, and $\sigma(\Delta + N \rightarrow \Delta + N)$ be the in-medium cross section.

Although the collective pionic modes can thus be effectively treated as ordinary particles, the fact that their wave functions contain components from π, NN^{-1} and ΔN^{-1} states makes it difficult to picture them in a physically simple manner. Fortunately, their specific structure is not important for the transport process, as as long as these quasiparticles remain well inside the nuclear medium. First when such a quasiparticle penetrates a nuclear surface and emerges as a free particle is it physically meaningful to determine what kind of real particle it is. The gradual transformation of the collective quasiparticle occurs automatically within the formalism, because as the density is lowered, $\rho \rightarrow 0$, a pionic mode will acquire 100% of either the pion component or the ΔN^{-1} component, depending on ω and q. That is to say, it will turn into either a free pion or an unperturbed ΔN^{-1} state. The squared amplitudes have their values between zero and unity and we therefore employ the parametrizations

$$Z^{\tilde{\pi}_1}(\boldsymbol{q};\rho)^2 \approx f_2(q, \vec{C}''[Z^{\tilde{\pi}_1}]); \tag{30}$$

$$Z^{\tilde{\pi}_2}(\boldsymbol{q};\rho)^2 \approx 1 - f_2(q, \vec{C}''[Z^{\tilde{\pi}_2}]) \tag{31}$$

$$\sum X^{\tilde{\pi}_1}_{\Delta N^{-1}}(\boldsymbol{q};\rho)^2 \approx 1 - f_2(q, \vec{C}''[X^{\tilde{\pi}_1}_{\Delta N^{-1}}]) \tag{32}$$

$$\sum X^{\tilde{\pi}_2}_{\Delta N^{-1}}(\boldsymbol{q};\rho)^2 \approx f_2(q, \vec{C}''[X^{\tilde{\pi}_2}_{\Delta N^{-1}}]) \ , \tag{33}$$

with $f_2(q, \vec{C}'')$ from eq. (29), while the sum of the squared NN^{-1} amplitudes are obtained from the normalization, *i.e.* all squared amplitudes sum up to unity. The density-dependent coefficients $\vec{C}''$, are presented in fig. 7. There remains the practical problem of how to represent an unperturbed ΔN^{-1} state when $\rho \rightarrow 0$. However, as will be discussed in section 4, only a very small fraction of the pionic modes (vanishing for a stationary density profile) will emerge as unperturbed ΔN^{-1} states.

Note that this approach is different from earlier works [8, 9, 12] where the nature of the pionic mode was determined already in the creation process, *i.e.* when the mode was created it was determined whether it represented a free pion or an unperturbed ΔN^{-1} state. This difference in approach will have crucial effects for the collective modes that escape the system, as will be seen in the next sections.

4 Quasipions at the nuclear surface

In previous works the quasipions at a surface have been treated in various approximations. In ref. [8] effective dispersion relations were introduced, corresponding to

modes with either 100% pionic or ΔN^{-1} component. The pionic mode was then propagated as a quasipion, emerging as a free pion at the surface, while the ΔN^{-1} mode was used to derive a Δ potential for the uncoupled Δs. In this way only pions and Δs escape the system, but the drawback is that the effective dispersion relations are quite distorted compared to the original ones, and that the in-medium effects seem to be over-estimated by allowing all uncoupled Δs propagate in a collective potential.

In [9] both collective modes were propagated, and hence some modes escape the system as unperturbed ΔN^{-1} states. This was effectively taken care of by converting these modes to free Δs (neglecting baryon number conservation), with the justification that the number of modes escaping the system as unperturbed ΔN^{-1} states were found to be small. We will in this paper report on alternative ways to treat the modes at the surface based on ref. [10], and how this treatment can improve the descriptions in refs. [8, 9].

We first consider the simplified case when the nuclear surface is stationary *i.e.* $\rho(\boldsymbol{r}, t) = \rho(\boldsymbol{r}, 0)$ for all times t. This means that there is no explicit time dependence in the effective Hamiltonians in equation (20), and thus the energies of the collective pionic modes are conserved. For a pionic mode with energy $\hbar\omega_\nu(\boldsymbol{q}; \rho)$ propagating in a varying density this means that the momentum $\boldsymbol{q}$ will change as ρ changes. That is to say, the pionic mode effectively feels a potential. In addition to momentum changes, also the amplitudes $X^\nu_{jk}(\boldsymbol{q}; \rho)$, $Z^\nu(\boldsymbol{q}; \rho)$ and $W^\nu(\boldsymbol{q}; \rho)$ of the baryon-hole and pion components will change as the density changes. In the limit of vanishing density either $X^\nu_{\Delta N^{-1}}$ or Z^ν will turn to unity, depending on the mode ν and its energy and momentum.

In the latter case no problems arise, the collective mode has simply been converted to a free pion escaping the system. However, in the former case there is some inconsistency in the formalism since there are no hole states in vacuum ($\rho = 0$). In a quantal description of spin-isospin modes propagating at a surface different scenarios could emerge. There is some small probability that the mode could be reflected at the surface. Alternatively the mode could break up in an uncoupled Δ escaping the system, with the hole is trapped inside the nucleus. In a transport description this could be handled by allowing the test particle representing the mode ν to absorb a nearby nucleon, converting it into a Δ isobar.

We consider in this section the quasipions at a surface propagating from normal nuclear density to vacuum. In this case the amplitude W^ν will be very small and we will therefore omit it in the qualitative discussion of this section.

In fig. 8*a* we present the energy $\hbar\tilde{\omega}_1(\boldsymbol{q})$ of the lower collective mode $\tilde{\pi}_1$ for different densities in the range $0.1\rho^0 \leq \rho \leq \rho^0$. The line closest to the free pion relation (dotted line) represents the dispersion relation at the lowest density. As the density is increased the energy relation is (for each fixed q) lowered. For small q values the mode is completely dominated by the pion component. As q is increased also the ΔN^{-1} components starts to contribute substantially (although to different extent depending on the density). In the approximate range 300 MeV/$c \leq q \leq$ 400 MeV/c (depending on density) the mode enters the ΔN^{-1} continuum and changes character from collective mode to non-collective.

We will in this section discuss four different examples, suitably chosen to illustrate

the main features.

4.1 Lower pionic mode

In our first example we consider the mode $\tilde{\pi}_1$ created at normal density with energy $\hbar\tilde{\omega}_1 = 200$ MeV propagating towards vacuum without any interactions. Initially this mode has the following characteristics:

$$q \approx 220 \text{ MeV}/c \quad |Z|^2 \approx 0.72 \quad \sum_{\Delta N^{-1}} |X_{\Delta N^{-1}}|^2 \approx 0.25 \quad \sum_{NN^{-1}} |X_{NN^{-1}}|^2 \approx 0.03 \ .$$

As the density decreases it will, due to the energy conservation, follow the path indicated by the dashed line in fig. 8*a*, from $q \approx 220$ MeV/c to $q \approx 150$ MeV/c. In fig. 9*a* we see how the squared amplitudes vary with the density for this particular energy of the mode $\tilde{\pi}_1$. As seen in fig. 9*a* only the pion component remains, as the zero density limit is reached. Thus in this particular case, the mode will escape the system as a free pion. In fig. 10*a* we show the squared amplitudes of the individual ΔN^{-1} amplitudes for the energy $\hbar\tilde{\omega}_1 = 200$ MeV of the mode $\tilde{\pi}_1$. We see that the mode is collective at all densities.

In the discussion so far we have not addressed the creation process. How probable is it that we produce the mode $\tilde{\pi}_1$ at the particular energy $\hbar\tilde{\omega}_1 = 200$ MeV? This information is given by the partial Δ decay width to the mode $\tilde{\pi}_1$. In fig. 11*a* we display the partial Δ decay width, $\tilde{\Gamma}^1_\Delta$, for different densities, as a function of the energy of the emitted quasipion $\tilde{\pi}_1$. Note that the width displayed in fig. 11*a* is for a Δ at rest, and that the Pauli blocking of the emitted nucleon has not been taken into account (the Pauli blocking is treated explicitly in a transport description). As seen in fig. 11*a* the width is quite substantial at the quasipion energy $\hbar\tilde{\omega}_1 = 200$ MeV, about 80 MeV compared to the free width, which is about 30 MeV at this energy. Thus it is quite probable for a Δ to decay to the mode $\tilde{\pi}_1$ around this quasipion energy.

Apart from penetrating the surface there is also some probability for the mode $\tilde{\pi}_1$ to be reflected at the surface. This is difficult to exactly predict since the reflection coefficient, $\mathcal{R}$, will depend on the actual density profile. However a first estimate can be obtained by considering a one-dimensional scenario with a density profile that corresponds to a Wood-Saxon potential with a surface thickness $a = 0.65$ fm. The height of the potential is then given by the change in the momentum of the pionic mode, and for the case of $\hbar\tilde{\omega}_1 = 200$ MeV we obtain $\mathcal{R} \approx 0.017$, see further the discussion in appendix A. This number is very small, which implies that the reflection can practically be neglected for this particular case. However, in other situations where the momentum change is different or the density profile is sharper, the reflection coefficient may be larger. We have therefore devoted appendix A to discuss how effective local reflection coefficients can be obtained and implemented in transport descriptions.

In our second example we also consider the mode $\tilde{\pi}_1$, but now with energy $\hbar\tilde{\omega}_1 = 295$ MeV. Initially this mode will now have the characteristics:

$$q \approx 450 \text{ MeV}/c \quad |Z|^2 \approx 0.0 \quad \sum_{\Delta N^{-1}} |X_{\Delta N^{-1}}|^2 \approx 0.94 \quad \sum_{NN^{-1}} |X_{NN^{-1}}|^2 \approx 0.06 \ .$$

As the density decreases it follows the path indicated by the dot-dashed line in fig. 8*a*, from $q \approx 450$ MeV/c to $q \approx 250$ MeV/c. In fig. 9*b* we see how the squared amplitudes vary with the density for this particular energy of the mode $\tilde{\pi}_1$. As seen in fig. 9*b* also in this case only the pion component remains, as the zero density limit is reached, although $\tilde{\pi}_1$ initially was completely dominated by the ΔN^{-1} component. Thus also in this case the mode will escape the system as a free pion.

In fig. 10*b* we show the squared amplitudes of the individual ΔN^{-1} amplitudes for the energy $\hbar\tilde{\omega}_1 = 295$ MeV of the mode $\tilde{\pi}_1$. Here the situation is different from the case at $\hbar\tilde{\omega}_1 = 200$ MeV, since initially the mode is dominated by a single ΔN^{-1} component, *i.e.* the mode is non-collective. However as the density is lowered the strength is spread over more ΔN^{-1} components and at low densities the mode is completely collective.

From fig. 11*a* we see that the partial width $\tilde{\Gamma}^1_\Delta$ is very close to zero at the quasipion energy $\hbar\tilde{\omega}_1 = 295$ MeV (dot-dashed curve) at normal nuclear density. Thus a Δ at normal nuclear density will not decay to a quasipion with this energy. The partial Δ width becomes very small because the collective strength, as well as the pion component, is negligible in this case. Although the mode at this energy cannot be created at normal nuclear density, it may still be created at lower densities, as can be seen in fig. 11*a*.

Making the same assumptions as in the first example, we find that the reflection coefficient, becomes smaller than 10^{-4} for this case.

We thus conclude that the lower pionic mode penetrating the surface will always emerge as a free pion. For low energies this is natural because as the density decreases the dispersion relation of the pionic mode approaches the free pion relation. The cases of sufficiently large energy to approach the unperturbed ΔN^{-1} branch as the density is lowered will never occur since no such modes will be created from a decaying Δ, because the partial Δ width will be zero.

4.2 Upper pionic mode

Also on the upper collective mode, $\tilde{\pi}_2$ a similar effect will occur. However some properties are somewhat different so we will therefore illustrate also this case with two typical examples. In our third example we thus consider the mode $\tilde{\pi}_2$, with energy $\hbar\tilde{\omega}_2 = 320$ MeV. Note that at this energy the mode can only exist at densities up to about $0.5\rho^0$. Initially, at $\rho = 0.5\rho^0$, this mode will have the characteristics:

$$q \approx 0 \text{ MeV}/c \quad |Z|^2 \approx 0.0 \quad \sum_{\Delta N^{-1}} |X_{\Delta N^{-1}}|^2 \approx 1.0 \quad \sum_{NN^{-1}} |X_{NN^{-1}}|^2 \approx 0.0 \; .$$

As the density decreases we follow the path indicated by the dashed line in fig. 8*b*, from $q \approx 0$ MeV/c to $q \approx 270$ MeV/c. Note that on the upper collective mode the momentum increases as the density decreases, corresponding to a negative potential step.

In fig. 9*c* we see how the squared amplitudes vary with the density for this particular energy of the mode $\tilde{\pi}_2$. As seen in fig. 9*c*, contrary to previous examples, only the ΔN^{-1} component remains, as the zero density limit is reached. In fig. 10*c* we show the squared amplitudes of the individual ΔN^{-1} amplitudes for the energy

$\hbar\tilde{\omega}_2 = 320$ MeV of the mode $\tilde{\pi}_2$. Initially the mode is collective, but as the density is lowered the mode becomes more and more non-collective. From fig. 11*b* we however see that the partial width $\tilde{\Gamma}^2_\Delta$ actually is zero at the quasipion energy $\hbar\tilde{\omega}_2 = 320$ MeV (dot-dashed curve) at all densities. Thus a Δ will not decay to a quasipion with this energy.

A mode at this energy with a very low momentum at half nuclear density, which could occur in a time-dependent density, could have a very large reflection coefficient, approaching unity as the initial quasipion momentum approaches zero.

In our fourth and last example in this section we consider the mode $\tilde{\pi}_2$ with energy $\hbar\tilde{\omega}_2 = 380$ MeV. Initially this mode will now have the properties:

$$q \approx 170 \text{ MeV}/c \quad |Z|^2 \approx 0.12 \quad \sum_{\Delta N^{-1}} |X_{\Delta N^{-1}}|^2 \approx 0.88 \quad \sum_{NN^{-1}} |X_{NN^{-1}}|^2 \approx 0.0 \; .$$

As the density decreases we follow the path indicated by the dot-dashed line in fig. 8*b*, from $q \approx 170$ MeV/c to $q \approx 350$ MeV/c. In fig. 9*d* we see how the squared amplitudes vary with the density for this particular energy of the mode $\tilde{\pi}_2$. As seen in fig. 9*d* in this case only the pion component remains, as the zero density limit is reached, although $\tilde{\pi}_2$ initially was dominated by the ΔN^{-1} component. Thus also in this case the mode will escape the system as a free pion.

In fig. 10*d* we show the squared amplitudes of the individual ΔN^{-1} amplitudes for the energy $\hbar\tilde{\omega}_2 = 380$ MeV of the mode $\tilde{\pi}_2$. We see that the mode at all densities is completely collective. From fig. 11*b* we see that the partial width $\tilde{\Gamma}^2_\Delta$ is quite substantial at the quasipion energy $\hbar\tilde{\omega}_2 = 380$ MeV (dot-dashed curve) also at normal nuclear density. The reflection coefficient, making the same assumptions as in the first example, becomes for this case smaller than 10^{-3}.

We thus conclude that also the upper pionic mode penetrating the surface will always emerge as a free pion. For high energies this is natural because as the density decreases the dispersion relation of the pionic mode approaches the free pion relation. The cases of low energy when the unperturbed ΔN^{-1} branch is approached as the density is lowered, will never occur since no such modes will be created from a decaying Δ, because the partial Δ width will be zero.

4.3 Refined scenarios

If the surface changes with time the energy of the pionic mode need not to be conserved, and there is some small possibility for the pionic mode to end up as an unperturbed Δ-hole state. The actual fraction of such modes is hard to estimate without an explicit transport simulation, but based on the scenario for the time-independent density profile, it is reasonable to expect that only a very small fraction of the pionic modes will end up as unperturbed Δ-hole states in vacuum.

In a quantum description such a mode could be either reflected at the surface, or the mode could break up into an uncoupled Δ and hole, where the hole is trapped inside the nucleus, and the Δ escape the system as a free Δ. Based on the results discussed in the explicit examples of this section, and the presentation in appendix A we expect that the reflection at the surface will be very small.

In a transport description the reflection can be incorporated by a local transmission coefficient as discussed in appendix A. If the pionic mode is not reflected at the surface, and its amplitude approaches 100% of the ΔN^{-1} component as the density approaches zero, the mode should thus break up into an uncoupled Δ and hole. In a transport simulation this could be practically handled by allowing the pionic mode to absorb a nearby nucleon, forming an uncoupled Δ, when the density falls below a specified value. This prescription has some quantum mechanical justification by the fact that at very low density a wave packet representing the pionic mode, will not be very well localized, but instead have a large spatial spread.

5 Summary

In-medium properties obtained in an infinite stationary system consisting of interacting nucleons, nucleon resonances and mesons, can be incorporated into transport descriptions by a local density approximation. While such a prescription is rather straightforward to implement in the interior regions of the nuclear system, conceptual problems exist at the nuclear surface. When the nuclear density approaches zero, collective mesonic modes formed in the medium have to be converted to real particles in vacuum. The problems arise since some collective modes (e.g. ΔN^{-1}-like) may exists in the infinite stationary system at arbitrary low (but non-vanishing) density, but no corresponding real particle exists in vacuum. This problem has been apparent in previous works [8, 9] where collective modes have been incorporated into transport descriptions as quasimesons. The character of the quasimesons (*i.e.* realization in vacuum) were in those works determined already at the time of creation.

Based on the formalism of ref. [10], we have in this paper employed a more elaborate $\pi + NN^{-1} + \Delta N^{-1}$ model (relative to the works [8, 9]) to investigate a somewhat different treatment of the collective pionic modes at a nuclear surface. In this formalism we have obtained not only density dependent dispersion relations of the pionic modes, but also density dependent amplitudes of the components constituting the pionic mode. These quantities are conveniently parametrized with density dependent parameters, in section 3.

For the transport process it is not needed to determine the character of the pionic modes until they penetrate the surface and emerge as free particles. This is automatically determined within our formalism from the amplitudes at zero density. We have further showed in section 4 that for a stationary density profile, the conservation of the energy of the pionic mode and the partial Δ decay width, together leads to the fact that only real pions are realized as free particles when the pionic mode penetrates the surface. Note that this finding is different from earlier works, and it demonstrates the importance of deriving dispersion relations and partial Δ widths consistently within a realistic[2] ΔN^{-1} model.

In a more refined scenario, where the density changes with time, deviations from this picture can be expected and also the unperturbed ΔN^{-1} component may be

[2]By "realistic" we here mean that the ΔN^{-1} model contains a continuum of ΔN^{-1} and NN^{-1} states, as compared to the more simple two-level ΔN^{-1} model used for example in refs. [8, 9].

realized in the limit of vanishing density. The actual fraction of such modes is hard to estimate without an explicit transport simulation, but based on the arguments in section 4 for the stationary surface, we expect this fraction to be very small.

For the rare cases when the unperturbed ΔN^{-1} component is realized in the limit of vanishing density, the pionic mode must be converted to real particles. In an extended description this could be made by allowing the mode to break up into an uncoupled Δ and a N^{-1}, where the hole remains trapped in the nuclear system and the Δ escapes the system. Based on our formalism, this seems to be the most probable scenario, since the collective strength disappears on these modes as the density approaches zero. This could be implemented in a transport simulation by letting the pionic mode absorb a nearby nucleon to form an uncoupled Δ, as may be justified by the quantum-mechanical feature that the wave packet representing the pionic mode is not well localized at very low density.

Alternatively the pionic modes could in a quantal description be reflected at the surface. We have investigated the reflection and transmission probabilities for the collective modes in a simplified one-dimensional scenario, where the modes propagate perpendicular to the surface. Exploring typical scenarios, we have found that (with only very few exceptions) the reflection of the pionic modes will be smaller than a few percent, however, in appendix A we have suggested how the reflection and transmission probabilities could be incorporated into the transport descriptions by using approximative local transmission coefficients.

Stimulating discussions with Volker Koch are acknowledged. This work was supported by the Swedish Natural Science Research Council, and by the Director, Office of Energy Research, Office of High Energy and Nuclear Physics, Nuclear Physics Division of the U.S. Department of Energy under Contract No. DE-AC03-76SF00098.

A Reflection and transmission at a surface

In the semi-classical transport descriptions all (test)particles are treated as classical particles. When such a classical particle propagates in a spatially varying potential its velocity will change. But assuming its energy exceeds the maximum value of the potential, the particle will continue to propagate through the varying potential. This is in contrast to a quantal description where the particle is represented by a wave packet. This wave packet has some probability to be reflected in a spatially varying potential. The reflection probability depends on several factors, such as the energy of the wave packet, and the height and shape of the potential.

In this section we investigate reflection and transmission probabilities in different idealized situations for a one-dimensional scenario, corresponding to the direction normal to the nuclear surface. We will also discuss how these effects could be approximately incorporated into transport descriptions. The treatment is intended to be used for the collective spin-isospin modes (quasi-pions) approaching a nuclear surface. The formalism, though, is quite general and could be applied also for other particles.

We will start to investigate some special cases when the potential is stationary. Subsequently we will discuss how the non-stationary case could be treated. In all cases we will assume that the potential is constant outside a finite interval,

$$V(x) = \begin{cases} 0 & x < x_L \\ V(x) & x_L < x < x_R \\ V_0 & x_R < x \end{cases} . \tag{34}$$

For $x < x_L$ we have an incoming wave and we ask for the probability that we have an outgoing wave at $x > x_R$, *i.e.* we seek the transmission and reflection coefficients, $\mathcal{T}$ and $\mathcal{R}$ respectively, with $\mathcal{T} + \mathcal{R} = 1$. Only for some special simple forms of the potential $V(x)$ can the coefficients $\mathcal{R}$ and $\mathcal{T}$ be obtained analytically.

Note that both the stationary Schrödinger equation

$$\left[-\frac{\hbar^2}{2m}\frac{d^2}{dx^2} + V(x) \right] \psi(x) = E\psi(x) \tag{35}$$

and the stationary Klein-Gordon equation

$$\left[\hbar^2 c^2 \frac{d^2}{dx^2} + \hbar^2\omega^2 - m^2c^4 \right] \psi(x) = 2\hbar\omega V(x)\psi(x) \tag{36}$$

for a particle with energy $E = \hbar\omega$, can be rewritten in the form

$$\left[\frac{d^2}{dx^2} + k(x)^2 \right] \psi(x) = 0 . \tag{37}$$

by introducing a local wave number

$$k(x) = \sqrt{2m[E - V(x)]}/\hbar , \tag{38}$$

or

$$k(x) = \sqrt{\hbar^2\omega^2 - m^2c^4 - 2\hbar\omega V(x)]}/\hbar c , \tag{39}$$

respectively. The results obtained in the sequel in this section are derived using the Schrödinger equation, but from eqs. (35) to (37) it follows that the results are valid also for a particle described by the Klein-Gordon equation, if the local wave number is taken according to equation (39) instead of equation (38).

The simplest case is a potential step at $x = 0$,

$$V(x) = \begin{cases} 0 & x < 0 \\ V_0 & 0 < x \end{cases} . \tag{40}$$

This case can be found in elementary textbooks on quantum mechanics. Here we briefly recapitulate the main steps as a preparation for more complicated cases. The Schrödinger equation has the solution

$$\psi(x) = \begin{cases} \frac{A}{\sqrt{k_L}}e^{ik_Lx} + \frac{B}{\sqrt{k_L}}e^{-ik_Lx} & x < 0 \\ \frac{C}{\sqrt{k_L}}e^{ik_Rx} + \frac{D}{\sqrt{k_L}}e^{-ik_Rx} & 0 < x \end{cases} , \tag{41}$$

where $k_L = \sqrt{2mE}/\hbar$ and $k_R = \sqrt{2m(E-V_0)}/\hbar$, for a particle with energy $E > V_0$. Taking only an outgoing solution at $x > x_R$ (*i.e.* $D = 0$), and relating the coefficients A, B and C by a smooth joining at $x = 0$,

$$\begin{cases} \psi(0-\epsilon) = \psi(0+\epsilon) \\ \psi'(0-\epsilon) = \psi'(0+\epsilon) \end{cases} , \tag{42}$$

the reflection and transmission coefficients are obtained as

$$\begin{aligned} \mathcal{R} &= \frac{|B|^2}{|A|^2} = \frac{(k_L - k_R)^2}{(k_L + k_R)^2} \\ \mathcal{T} &= \frac{|C|^2}{|A|^2} = \frac{4k_L k_R}{(k_L + k_R)^2} . \end{aligned} \tag{43}$$

Also for other special forms of the potential can the reflection and transmission coefficients be derived analytically, such as for the Woods-Saxon type of potential,

$$V(x) = V_0/[1 + \mathrm{e}^{-x/a}] . \tag{44}$$

Here the reflection coefficient $\mathcal{R}$ is given by [13]

$$\mathcal{R} = \left(\frac{\sinh[a\pi(k_L - k_R)]}{\sinh[a\pi(k_L + k_R)]} \right)^2 , \tag{45}$$

and the transmission coefficient is obtained from $\mathcal{T} = 1 - \mathcal{R}$. Note that the case of the potential step, eq. (40), emerges in the limit $a \to 0$.

For an arbitrary potential the coefficients $\mathcal{R}$ and $\mathcal{T}$ do not have an analytical form. An approximate solution can be obtained by approximating the potential $V(x)$ by a piecewise constant potential

$$V(x) = \begin{cases} 0 & x < x_0 = x_L \\ V(x) \approx \sum_{j=0}^{n-1} V_j(x) & x_0 = x_L < x < x_n = x_R \\ V_0 & x_N = x_L < x \end{cases} , \tag{46}$$

with

$$V_j(x) = V(x_j + \Delta x/2)[\theta(x_{j+1} - x) - \theta(x_j - x)], \quad \begin{cases} x_j &= x_L + j\,\Delta x \\ \Delta x &= [x_R - x_L]/n \end{cases} , \tag{47}$$

and by making the ansatz,

$$\psi(x) \approx \sum_{j=0}^{n-1} \psi_j(x)[\theta(x_{j+1} - x) - \theta(x_j - x)] \qquad x_0 = x_L < x < x_n = x_R , \tag{48}$$

with

$$\psi_j(x) = \frac{A_j}{\sqrt{k_j}} \mathrm{e}^{ik_j x} + \frac{B_j}{\sqrt{k_j}} \mathrm{e}^{-ik_j x} \tag{49}$$

and

$$k_j = \sqrt{2m[E - V(x_j + \Delta x/2)]}\hbar \ . \tag{50}$$

The coefficients A_j and B_j are determined from the condition of smooth joining,

$$\begin{cases} \psi_j(x_{j+1} - \epsilon) = \psi_{j+1}(x_{j+1} + \epsilon) \\ \psi'_j(x_{j+1} - \epsilon) = \psi'_{j+1}(x_{j+1} + \epsilon) \end{cases} \ , \qquad \epsilon \to 0^+ \ , \tag{51}$$

and the boundary condition of an outgoing solution at $x > x_R$, *i.e.* $A_{n-1} = 1$ and $B_{n-1} = 0$. Not that in the especially simple case of no reflection, the ansatz above becomes identical to the WKB approximation, in which the the coefficients A_j and B_j are constants, *i.e.* $A_j \equiv A$ and $B_j \equiv B$ for all j.

The transmission coefficient, $\mathcal{T}$, is obtained from

$$\mathcal{T} = \frac{|A_{n-1}|^2}{|A_0|^2} \ , \tag{52}$$

and $\mathcal{R} = 1 - \mathcal{T}$. We have numerically checked that for the Woods-Saxon type of potential above, this approximation procedure, with a very high accuracy, yields the same reflection and transmission coefficients as the analytical result. We have compared the analytical and numerical results for many different energies (E) and parameters of the potential (V_0, a), and only for E very close to V_0 are there deviations larger than a few percent.

In a heavy-ion collision the potential is not stationary, but changes with the time. The formalism above can be generalized to a time-dependent potential. The particles to be propagated are in a quantal description represented by wave packets. We therefore generalize the definition of the transmission coefficient to be valid also for a propagating wave packet in a non-stationary potential. As before we assume that we have an incident wave or wave packet, $\psi_{\rm inc}(x,t)$, at $x = x_L$. We associate a probability current with this wave packet by

$$j_{\rm inc}(x,t) = \frac{\hbar}{m} \ {\rm Im} \ \left(\frac{d\psi_{\rm inc}(x)}{dx} \ \psi_{\rm inc}(x)^* \right) \tag{53}$$

Similarly we assume that we have an outgoing wave or wave packet, $\psi_{\rm out}(x,t)$, at $x = x_R$, and we associate a probability current, $j_{\rm out}(x,t)$, with this wave packet. A transmission coefficient can then be defined as the ratio between the outgoing probability flowing through the point x_R and the incident probability flowing through the point x_L,

$$\mathcal{T} = \frac{\int_{t_1}^{t_2} j_{\rm out}(x_R,t)dt}{\int_{t_1}^{t_2} j_{\rm inc}(x_L,t)dt} \tag{54}$$

where the times t_1 and t_2 are chosen such that a wave packet will propagate through both the points x_L and x_R within the time interval. Note that this definition of $\mathcal{T}$ agrees with the results stated for the stationary case. By solving the time-dependent Schrödinger equation numerically, and expanding a wave packet in this basis set, a transmission coefficient could in principle be obtained from eq. (54) for an arbitrary

(known) potential $V(x,t)$. In a transport description, however, the potential $V(x,t)$ is not known in advance, and the described method is not so useful. Instead it would be more useful with a local transmission coefficient $t(x_j)$, which would give the probability for the wave packet to be transmitted from the point x_j to the point $x_{j+1} = x_j + \Delta x$, where the total transmission coefficient is given by $\mathcal{T} = \prod_{j=0}^{n-1} t(x_j)$. Such a local coefficient can formally be obtained by writing

$$\mathcal{T} = \mathrm{e}^{-\int_{x_L}^{x_R} r(x)dx} , \tag{55}$$

and by approximating the integral in the exponent by a discrete sum,

$$\mathcal{T} \approx \mathrm{e}^{-\sum_{j=0}^{n-1} r(x_j)\Delta x} = \prod_{j=0}^{n-1} \mathrm{e}^{-r(x_j)\Delta x} = \prod_{j=0}^{n-1} t(x_j) . \tag{56}$$

However, also in this expression the local reflection coefficient $r(x)$ will depend on the particle energy, and the shape and magnitude of the potential, and it is therefore not straightforward to implement a local transmission coefficient into a transport description.

It is therefore our strategy to approximate the function $r(x)$ with a relative simple expression depending on a few parameters, that are adjusted such that eq. (55) will yield a good approximation to the total transmission coefficient for a large class of realistic particle energies and potential parameters. We have empirically found that the ansatz

$$r(x) = \frac{C_1}{k(x)} \left(\frac{d \ln k(x)}{dx} \right)^2 . \tag{57}$$

with $C_1 \approx 0.116$, yields a good approximation for a range of different particle energies and a range of different values of a and V_0 in the Woods-Saxon type of stationary potential. In fig. 12 we present some examples of this approximation, compared to the analytical solutions.

As was discussed in section 4 it is only in rather few and special cases that the transmission coefficient for the collective pionic modes will deviate substantially from unity. We therefore conclude this section by summarizing that the reflection of pionic modes can be approximately incorporated into transport descriptions by an approximate local transmission coefficient

$$t(x) \approx \exp[-\frac{C_1}{k(x)} \left(\frac{d \ln k(x)}{dx} \right)^2 \Delta x] . \tag{58}$$

The error in this approximation is in most realistic cases smaller than 10%. Those events where a larger error may occur for pionic modes at a nuclear surface are expected to be very rare in transport simulations. Thus the total error in a transport treatment by using a local transmission coefficient according to eqs. (56) and (58) should be very small. However, the importance of incorporating the effects of reflection of pionic modes at the surface seems to be quite small, since in most events the total transmission coefficient will be close to unity.

B RPA equations for spin-isospin interaction

In this section we recapitulate the RPA equations, derived in ref. [10], in the spin longitudinal channel for the case when $T = 0$ and the Δ width is omitted in the RPA equations.

The spin-isospin excitations are characterized by the momentum $\boldsymbol{q}$ and the isospin λ. The energy of the spin-isospin modes are obtained from the determinant of the equation

$$\begin{pmatrix} 1 + \mathcal{W}^{NN}\mathcal{M}^N\Phi^N & \mathcal{W}^{N\Delta}\mathcal{M}^\Delta\Phi^\Delta \\ \mathcal{W}^{\Delta N}\mathcal{M}^N\Phi^N & 1 + \mathcal{W}^{\Delta\Delta}\mathcal{M}^\Delta\Phi^\Delta \end{pmatrix} \begin{pmatrix} x^N \\ x^\Delta \end{pmatrix} = 0 \,, \tag{59}$$

while the amplitudes are obtained from the solution of eq. (59),

$$Z = \frac{1}{\hbar\omega_\pi - \hbar\omega}\left[\mathcal{M}^N v_\pi^N \Phi^N x^N + \mathcal{M}^\Delta v_\pi^\Delta \Phi^\Delta x^\Delta\right] \tag{60}$$

$$W = \frac{1}{\hbar\omega_\pi + \hbar\omega}\left[\mathcal{M}^N v_\pi^N \Phi^N x^N + \mathcal{M}^\Delta v_\pi^\Delta \Phi^\Delta x^\Delta\right] \,, \tag{61}$$

and

$$X_{jk}(\omega, \boldsymbol{q}, \lambda) = \left(\frac{\hbar c}{L}\right)^{3/2} \frac{x(t_j, t_k;\, \boldsymbol{q};\, \lambda,\, \omega)}{e_{t_j}(\boldsymbol{p}_k + \boldsymbol{q}) - e_{t_k}(\boldsymbol{p}_k) + \Sigma_{jk} - \hbar\omega}\, \vartheta_{jk}(\hat{q}, -\lambda) \,, \tag{62}$$

with

$$\begin{aligned} x(1/2, 1/2;\, \boldsymbol{q};\, \lambda,\, \omega) &\equiv x^N \\ x(1/2, 3/2;\, \boldsymbol{q};\, \lambda,\, \omega) &= x(3/2, 1/2;\, \boldsymbol{q};\, \lambda,\, \omega) \equiv x^\Delta \\ x(3/2, 3/2;\, \boldsymbol{q};\, \lambda,\, \omega) &\equiv 0 \end{aligned}$$

and analogously for other quantities. In the above expressions $\alpha, \beta = N, \Delta$, and we have used the notations

$$\mathcal{W}^{\alpha\beta} = \frac{f_{N\alpha}^\pi f_{N\beta}^\pi}{(m_\pi c^2)^2}\left[\,|F_g|^2 g'_{\alpha\beta} + R_i^\alpha R_i^\beta |F_\pi|^2 (c\boldsymbol{q}_i)^2 D_\pi^0\,\right], \tag{63}$$

$$v_\pi^\alpha(\boldsymbol{q}, \omega) = i\, R_i^\alpha F_\pi \frac{f_{N\alpha}^\pi}{m_\pi c^2} \frac{|c\boldsymbol{q}_{cm}|}{\sqrt{2\hbar\omega_\pi(\boldsymbol{q})}} \tag{64}$$

$$R_\alpha^i(q)^2 = \frac{2m_\alpha c^2}{m_\alpha c^2 + \sqrt{s_i}} \tag{65}$$

$$\sqrt{s} = (E_N(\boldsymbol{p}_N) + \hbar\omega)^2 - (c\boldsymbol{q} + c\boldsymbol{p}_N)^2 \tag{66}$$

$$\approx (m_N c^2 + \ \mathrm{Re}\ \hbar\omega)^2 - c(\boldsymbol{q})^2 \equiv \sqrt{s_i} \tag{67}$$

$$\boldsymbol{q}_{cm} \approx \boldsymbol{q}_i = \frac{m_N c^2}{m_N c^2 + \hbar\omega}\boldsymbol{q} \,. \tag{68}$$

The numerical factors $\mathcal{M}^N = 4$ and $\mathcal{M}^\Delta = 16/9$ originates from the spin-isospin summation, and we have defined the Lindhard functions

$$\Phi^N(\omega, \boldsymbol{q}) = \left(\frac{\hbar c}{L}\right)^3 \sum_{\boldsymbol{p}} \frac{n(\boldsymbol{p}) - n(\boldsymbol{p} + \boldsymbol{q})}{(\boldsymbol{p} + \boldsymbol{q})^2/2m_N^* - \boldsymbol{p}^2/2m_N^* - \hbar\omega} \tag{69}$$

$$\Phi^{\Delta}(\omega,\boldsymbol{q}) \;=\; \Phi(\frac{1}{2},\frac{3}{2};\,\omega,\boldsymbol{q})+\Phi(\frac{3}{2},\frac{1}{2};\,\omega,\boldsymbol{q}) = \left(\frac{\hbar c}{L}\right)^3 \sum_{\boldsymbol{p}} \left\{ \frac{n(\boldsymbol{p})}{\delta e^{+}_{\Delta N}} + \frac{n(\boldsymbol{p})}{\delta e^{-}_{\Delta N}} \right\} \quad (70)$$

with

$$\delta e^{+}_{\Delta N} \;=\; \frac{(\boldsymbol{p}^{+}_{\Delta})^2}{2m_{\Delta}} - \frac{\boldsymbol{p}^2}{2m^{*}_{N}} + \Delta m + V^{\rm eff}_{\Delta}(\varepsilon^{+}_{\Sigma},\boldsymbol{p}^{+}_{\Delta}) - \hbar\omega \quad (71)$$

$$\delta e^{-}_{\Delta N} \;=\; \frac{(\boldsymbol{p}^{-}_{\Delta})^2}{2m_{\Delta}} - \frac{\boldsymbol{p}^2}{2m^{*}_{N}} + \Delta m + V^{\rm eff}_{\Delta}(\varepsilon^{-}_{\Sigma},\boldsymbol{p}^{-}_{\Delta}) + \hbar\omega \quad (72)$$

$$\Delta m = m_{\Delta} - m_N; \qquad \varepsilon^{\pm}_{\Sigma} = m_N + \frac{\boldsymbol{p}^2}{2m^{*}_{N}} \pm \hbar\omega; \qquad \boldsymbol{p}^{\pm}_{\Delta} = \boldsymbol{p} \pm \boldsymbol{q}\,. \quad (73)$$

The quantities x^N and x^{Δ} are determined from the normalization of the RPA states

$$\begin{aligned} \pm 1 \;&=\; \mathcal{M}^N \eta_N x^{*}_N x_N + \mathcal{M}^{\Delta}\eta_{\Delta} x^{*}_{\Delta} x_{\Delta} + Z^{*}Z - W^{*}W \\ &=\; x^{*}_N x_N \left(\mathcal{M}^N \eta_N + \left[\frac{1+\mathcal{W}^{NN}\mathcal{M}^N\Phi^N}{\mathcal{W}^{N\Delta}\mathcal{M}^{\Delta}\Phi^{\Delta}} \right]^2 \mathcal{M}^{\Delta}\eta_{\Delta} \right. \qquad (74) \\ &-\; \left. \left[\frac{1}{(\hbar\omega_{\pi}-\hbar\omega)^2} - \frac{1}{(\hbar\omega_{\pi}+\hbar\omega)^2} \right] \left\{ \mathcal{M}^N v^N_{\pi}\Phi^N - \frac{1+\mathcal{W}^{NN}\mathcal{M}^N\Phi^N}{\mathcal{W}^{N\Delta}} v^{\Delta}_{\pi} \right\}^2 \right) \end{aligned}$$

with

$$\eta_N(\omega,\boldsymbol{q}) \;=\; \left(\frac{\hbar c}{L}\right)^3 \sum_{\boldsymbol{p}} \frac{n(\boldsymbol{p}) - n(\boldsymbol{p}+\boldsymbol{q})}{[\frac{(\boldsymbol{p}+\boldsymbol{q})^2}{2m^{*}_{N}} - \frac{\boldsymbol{p}^2}{2m^{*}_{N}} - \hbar\omega]^2} = \frac{\partial}{\partial\hbar\omega}\Phi_N(\omega,\boldsymbol{q}) \quad (75)$$

$$\eta_{\Delta}(\omega,\boldsymbol{q}) \;=\; \left(\frac{\hbar c}{L}\right)^3 \sum_{\boldsymbol{p}} \left\{ \frac{n(\boldsymbol{p})}{[\delta e^{+}_{\Delta N}]^2} - \frac{n(\boldsymbol{p})}{[\delta e^{-}_{\Delta N}]^2} \right\} = \frac{\partial}{\partial\hbar\omega}\Phi_{\Delta}(\omega,\boldsymbol{q})\,, \quad (76)$$

and where we have assumed $\partial V^{\rm eff}_{\Delta}/\partial\hbar\omega \approx 0$.

The factor $h(jk;\nu)$, motivated in eq. (16), can using the RPA solution be explicitly expressed as

$$\begin{aligned} h(jk,\nu;\omega,\boldsymbol{q}) \;&=\; \sum_{\alpha=N,\Delta} \mathcal{M}_{\alpha}\Phi_{\alpha}(\omega_{\nu})x_{\alpha}(\omega_{\nu}) \left[(\hat{\boldsymbol{q}}_{jk}\cdot\hat{\boldsymbol{q}}_i) v^{\alpha,jk}_{B}(\omega) \right. \\ &\left. -\; 2\hbar\omega_{\pi} D^{0}_{\pi}(\omega_{\nu}) v^{jk}_{\pi}(\omega) v^{\alpha}_{\pi}(\omega_{\nu}) \right]\,, \qquad (77) \end{aligned}$$

where

$$v^{\alpha,jk}_{B}(\omega,\boldsymbol{q}) = g'_{\alpha,jk} \frac{f^{\pi}_{N,\alpha} f^{\pi}_{N,jk}}{(m_{\pi}c^2)^2}\; F^2_g(\omega,\boldsymbol{q})\,. \quad (78)$$

References

[1] V. Metag, Nucl. Phys. **A533** (1993) 283c.

[2] W. Cassing, V. Metag, U. Mosel, and K. Niita, Phys. Rep. **188** (1990) 363.

[3] U. Mosel, Ann. Rev. Nucl. Part. Sci. **41** (1991) 29.

[4] Gy. Wolf, G. Batko, W. Cassing, U. Mosel, K. Niita, and M. Schäfer, Nucl. Phys. **A517** (1990) 615.

[5] J. Aichelin, Phys. Reports **202** (1991) 233.

[6] G.E. Brown, E. Oset, M. Vincente Vacas, and W. Weise, Nucl. Phys. **A505** (1989) 823.

[7] G.F. Bertsch, G.E. Brown, V. Koch, and B.-A. Li, Nucl. Phys. **A490** (1988) 745.

[8] W. Ehehalt, W Cassing, A. Engel, U. Mosel, and Gy. Wolf, Phys. Lett. **298B** (1993) 31.

[9] L. Xiong, C. M. Ko, and V. Koch, Phys. Rev. **C47** (1993) 788.

[10] J. Helgesson and J. Randrup, Ann. Phys. (N.Y.) (Oct. 1995).

[11] E. Oset, H. Toki, and W. Weise, Phys. Reports **83** (1982) 281.

[12] V. Koch, private communication.

[13] L. D. Landau and E. M. Lifshits "Quantum Mechanics, Non-Relativistic Theory" Pergamon Press, 1965.

$m_N = 940$ MeV/c^2	$g'_{NN} = 0.9$	$f^{\pi}_{NN} = 1.0$
$m_\Delta = 1230$ MeV/c^2	$g'_{N\Delta} = 0.38$	$f^{\pi}_{N\Delta} = 2.2$
$m_\pi = 140$ MeV/c^2	$g'_{\Delta\Delta} = 0.35$	$f^{\pi}_{\Delta\Delta} = 0$
$\Lambda_g = 1.5$ GeV	$\Lambda^\pi = 1.0$ GeV	$\rho_0 = 0.153$ fm^{-3}
$V_\Delta - V_N = 25.0\rho/\rho_0$ MeV	$m^*_N = m_N/[1 + 0.4049(\rho/\rho_0)]$	

Table 1: Parameter values used in the numerical calculations.

Figure 1:
Diagrammatic representations of the Δ self energy Σ_Δ (left-hand side) and the partial Δ decay width to the particular spin-isospin mode ν, Γ^ν_Δ (right-hand side).

Figure 2:
The dispersion relations for the spin-isospin modes in the spin-longitudinal channel, in infinite nuclear matter at normal nuclear density and zero temperature. The non-collective modes are shown by solid curves, while collective modes $\tilde{\pi}_1$ and $\tilde{\pi}_2$ are represented by dot-dashed curves. As a reference, the free pion dispersion relation $\hbar\omega_\pi(q) = [(m_\pi c^2)^2 + (cq)^2]^{1/2}$, and the unperturbed ΔN^{-1} relation $\hbar\omega_{\Delta N^{-1}}(q) = m_\Delta c^2 - m_N c^2 + q^2/2m_\Delta$, are included as a dotted curves.

Figure 3:
The density-dependent parameters U_0 (solid curve), q_0 (dashed curve) and m_0 (dot-dashed) used in eq. (21) for fitting the dispersion relations of the lower collective mode $\tilde{\pi}_1$ (part a) and the upper collective mode $\tilde{\pi}_2$ (part b).

Figure 4:
The total Δ width $\Gamma^{\rm tot}_\Delta$ and its partial contributions from different spin-isospin modes for a Δ with momentum 300 MeV/c. The solid curve represents the total width, the long-dashed line is the contribution from the non-collective NN^{-1} modes, the short-dashed line is the contribution from the non-collective ΔN^{-1} modes, the dot-dashed line is the contribution from the lower pionic mode $\tilde{\pi}_1$, and the dot-dot-dashed line is the contribution from the upper pionic mode $\tilde{\pi}_2$. The intermediate nucleon in the Δ decay is not Pauli blocked. The error bars indicate the estimated uncertainty associated with the classification procedure (see ref. [10]).

Figure 5:
The density-dependent parameters, C_1 (dot-dashed curve), C_2 (short-dashed), C_3 (dot-dot-dashed) and C_4 (long-dashed), for the amplitudes of the ΔN^{-1} (part a) and the NN^{-1} (b) components on the lower pionic branch, eq. (24) and (25).

Figure 6:
The density-dependent parameters, C'_0 (part a), C'_1 (b), C'_{-1} (c) and C'_N (d), for the amplitudes of the ΔN^{-1} (long-dashed curve) and the NN^{-1} (dot-dashed) components on the upper pionic branch, eqs. (27) and (28).

Figure 7:
The density-dependent parameters, C_0'' (part a), C_1'' (b), and C_{-1}'' (c), for the squared amplitudes of the π (dot-dashed curve) and the ΔN^{-1} (short-dashed) components on the lower pionic branch, eqs. (30) and (32) and of the π (dot-dot-dashed) and the ΔN^{-1} (long-dashed) components on the upper pionic branch, eqs. (31) and (33).

Figure 8:
The energy $\hbar\tilde{\omega}(\boldsymbol{q})$ for different densities in the range $0.1\rho^0 \leq \rho \leq \rho^0$. In part a is presented the energies of the lower collective mode $\tilde{\pi}_1$ while the energies of the upper collective mode $\tilde{\pi}_2$ is shown in part b. As references the free pion dispersion relation and the unperturbed ΔN^{-1} relation have been plotted as dotted lines. The dashed and dot-dashed horizontal lines indicate the energies considered in the four examples of sections 4.1 and 4.2.

Figure 9:
Sum of all squared amplitudes of the ΔN^{-1} and NN^{-1} components, as well as squared amplitude of the pion component. In part a and b is shown the squared amplitudes for the lower pionic mode $\tilde{\pi}_1$ at the energies $\hbar\tilde{\omega}_1 = 200$ MeV and $\hbar\tilde{\omega}_1 = 295$ MeV, respectively. In c and d is displayed the squared amplitudes for the upper pionic mode $\tilde{\pi}_1$ at the energies $\hbar\tilde{\omega}_2 = 320$ MeV and $\hbar\tilde{\omega}_2 = 380$ MeV, respectively. The dot-dashed curve represents the pion component, the ΔN^{-1} component is represented by a short-dashed curve, and the long-dashed curve represents the NN^{-1} component.

Figure 10:
Squared amplitudes of the individual ΔN^{-1}, components. In part a and b is shown the squared amplitudes for the lower pionic mode $\tilde{\pi}_1$ at the energies $\hbar\tilde{\omega}_1 = 200$ MeV and $\hbar\tilde{\omega}_1 = 295$ MeV, respectively. In c and d is displayed the squared amplitudes for the upper pionic mode $\tilde{\pi}_2$ at the energies $\hbar\tilde{\omega}_2 = 320$ MeV and $\hbar\tilde{\omega}_2 = 380$ MeV, respectively.

Figure 11:
Partial Δ decay width for a Δ at rest, for different densities in the range $0.1\rho^0 \leq \rho \leq \rho^0$. In part a is presented the partial Δ width for the lower collective mode $\tilde{\pi}_1$ while the partial Δ width for the upper collective mode $\tilde{\pi}_2$ is shown in part b. As a reference the free Δ width has been plotted as a dotted line. The dashed and dot-dashed vertical lines indicate the energies considered in the four examples of sections 4.1 and 4.2.

Figure 12:
Total transmission coefficient, $\mathcal{T}$, obtained for a Woods-Saxon type of potential, eq. (44), for a range of potential parameters V_0 and a. The solid curve represents the exact expression, eq. (45), while the dashed curve represents the approximative result obtained from the local transmission coefficient, eqs. (56) and (58).

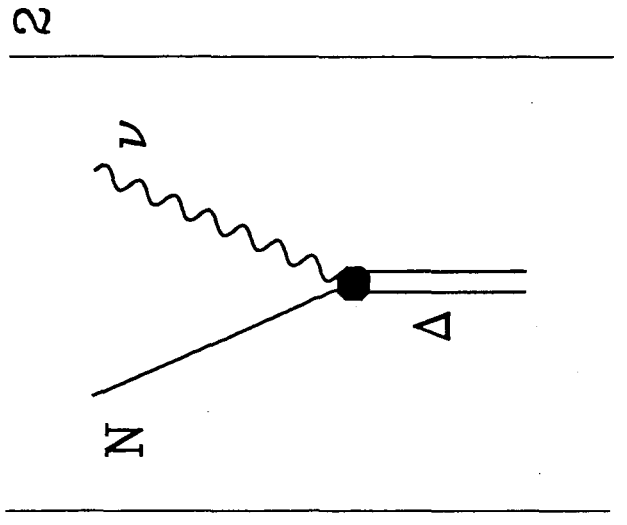

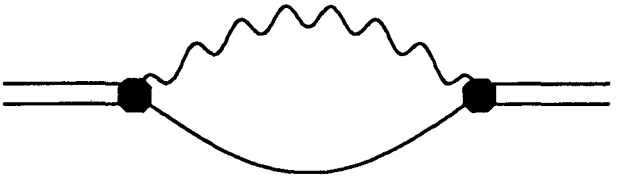

FIGURE 1

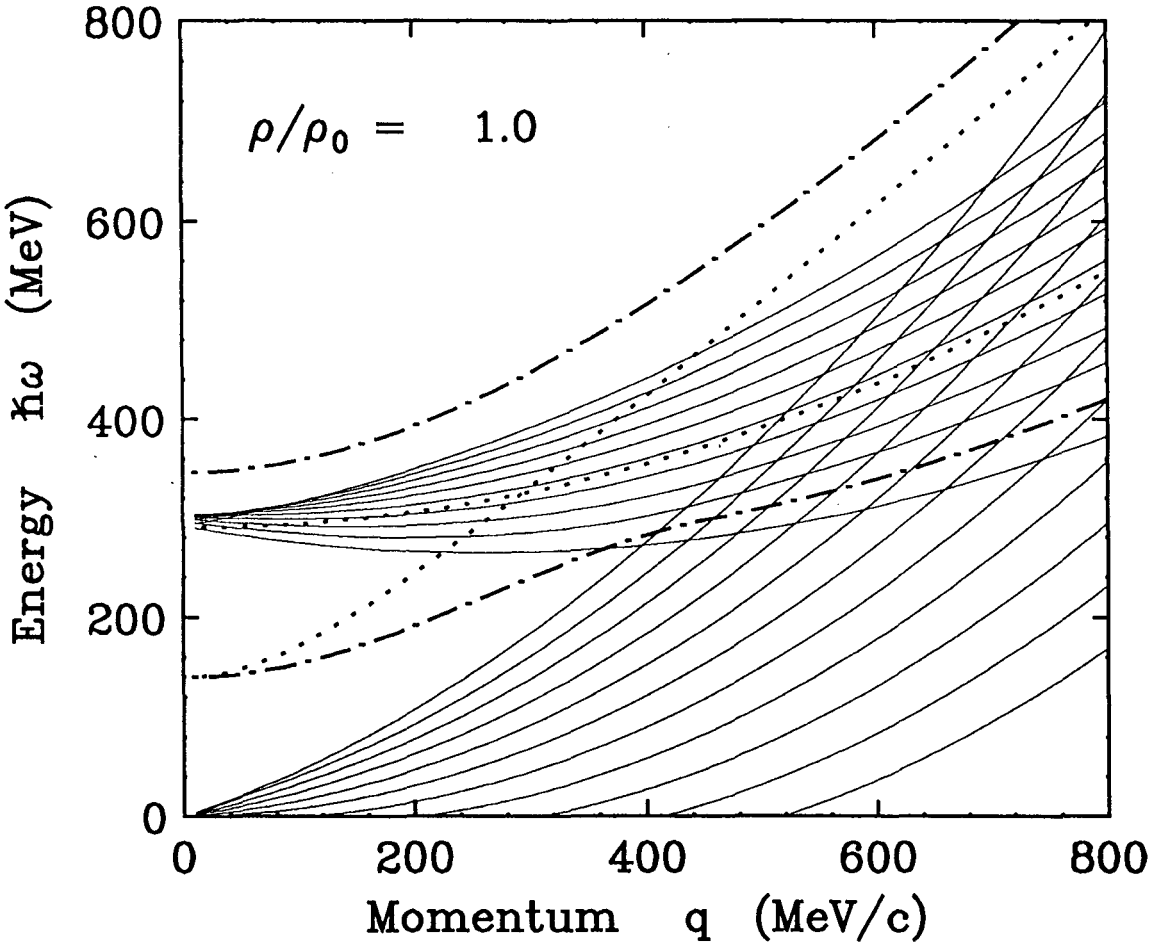
800
600
400
200
0
0
200
400
600
800
ρ/ρ_0 = 1.0
Energy $\hbar\omega$ (MeV)
Momentum q (MeV/c)

FIGURE 2

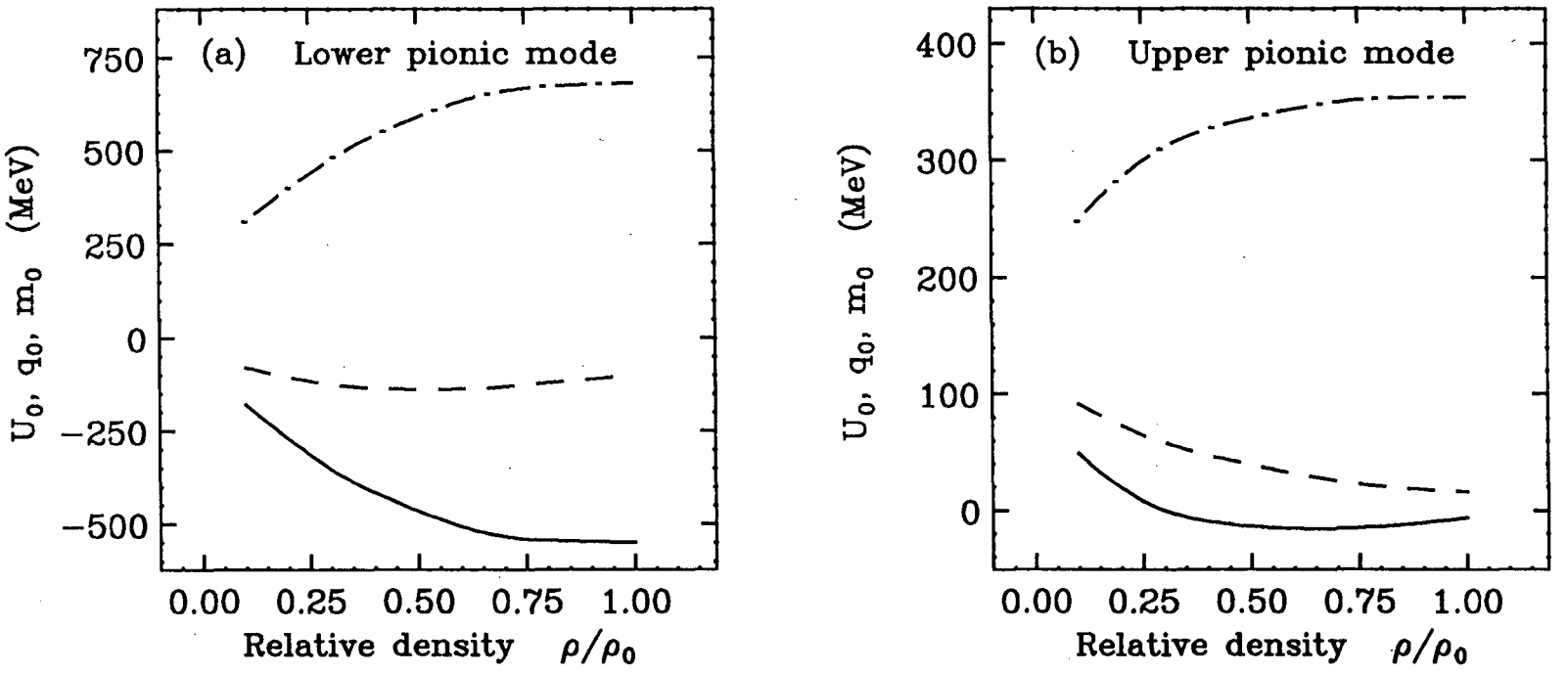
(a) Lower pionic mode
750
500
250
0
−250
−500
U_0, q_0, m_0 (MeV)
0.00 0.25 0.50 0.75 1.00
Relative density ρ/ρ_0
(b) Upper pionic mode
400
300
200
100
0
U_0, q_0, m_0 (MeV)
0.00 0.25 0.50 0.75 1.00
Relative density ρ/ρ_0

FIGURE 3

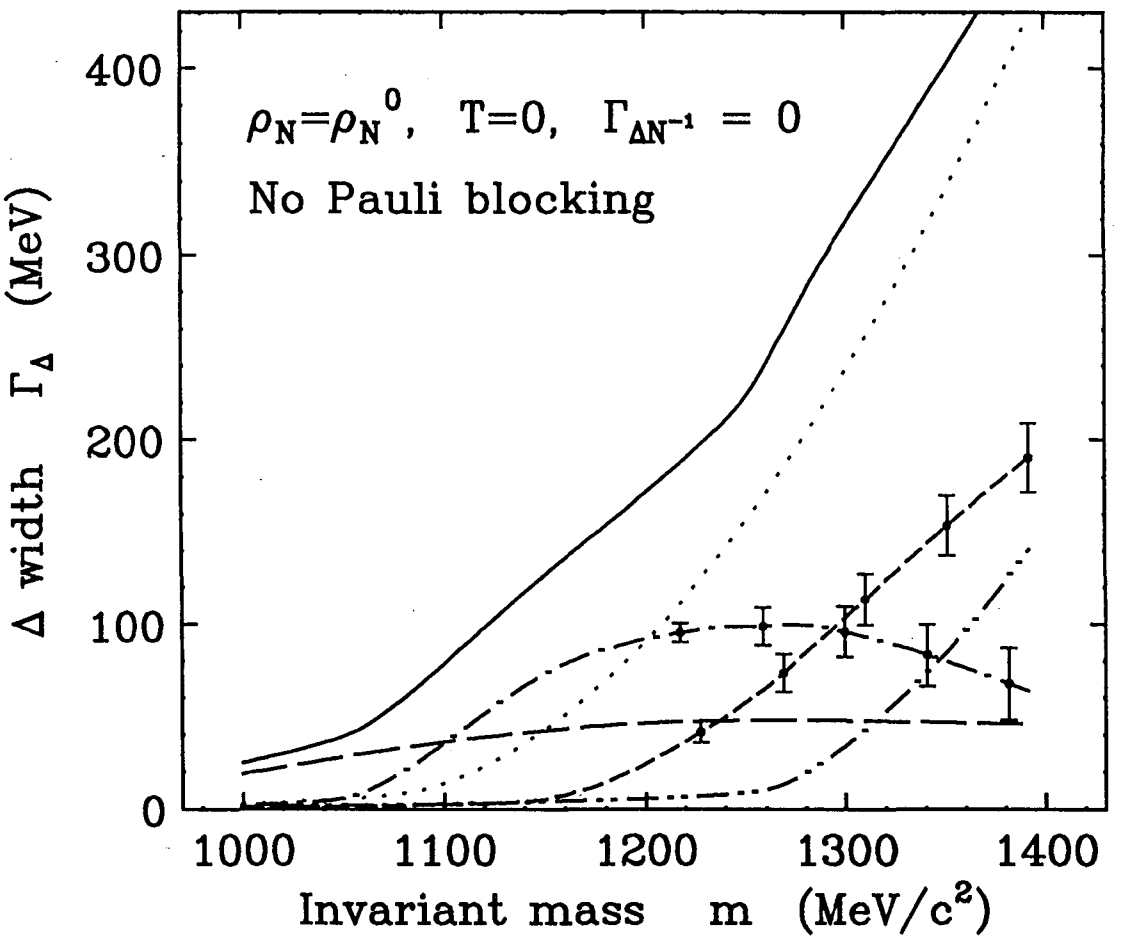
$\rho_N=\rho_N{}^0$, T=0, $\Gamma_{\Delta N^{-1}}$ = 0
No Pauli blocking
Δ width Γ_Δ (MeV)
400
300
200
100
0
1000
1100
1200
1300
1400
Invariant mass m (MeV/c^2)

FIGURE 4

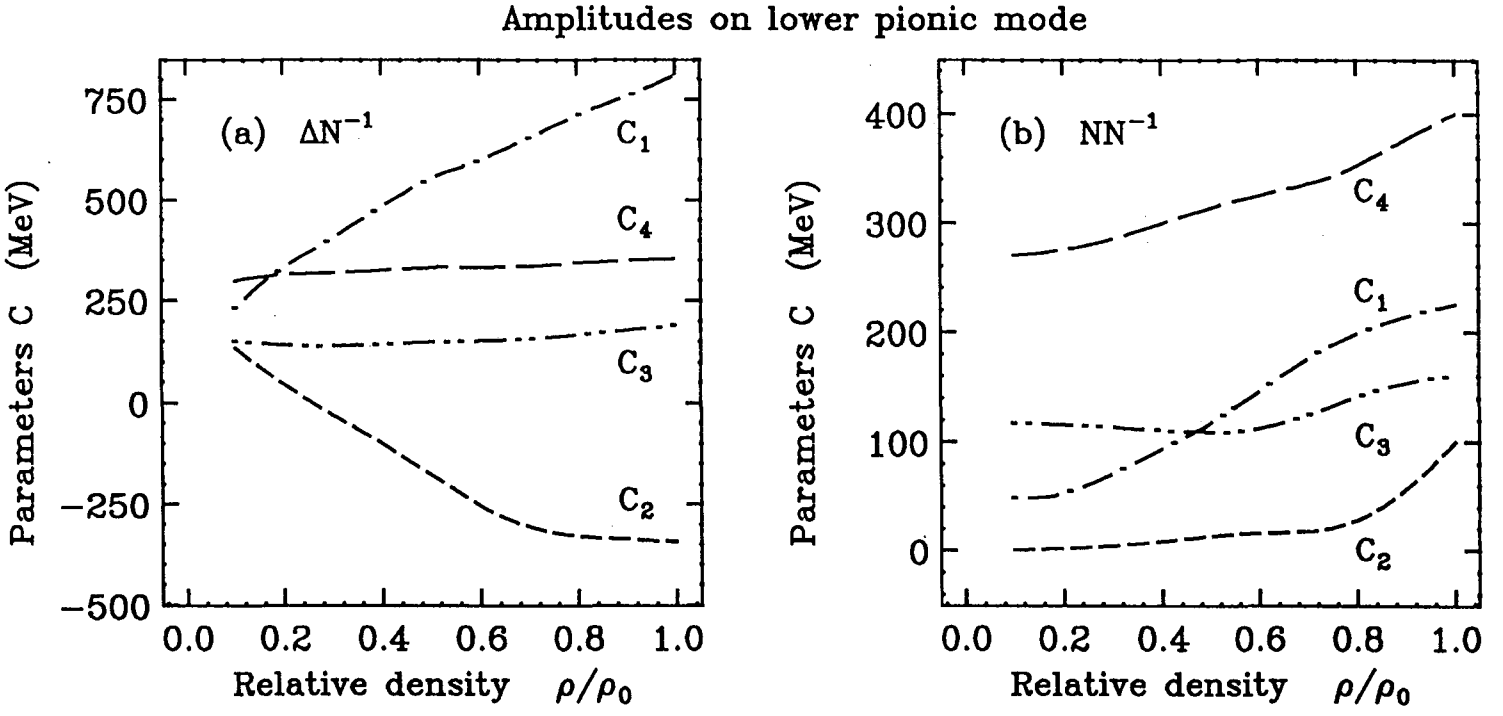
Amplitudes on lower pionic mode
(a) ΔN^{-1}
C_1
C_4
C_3
C_2
Parameters C (MeV)
750
500
250
0
−250
−500
0.0
0.2
0.4
0.6
0.8
1.0
Relative density ρ/ρ_0
(b) NN^{-1}
C_4
C_1
C_3
C_2
Parameters C (MeV)
400
300
200
100
0
0.0
0.2
0.4
0.6
0.8
1.0
Relative density ρ/ρ_0

FIGURE 5

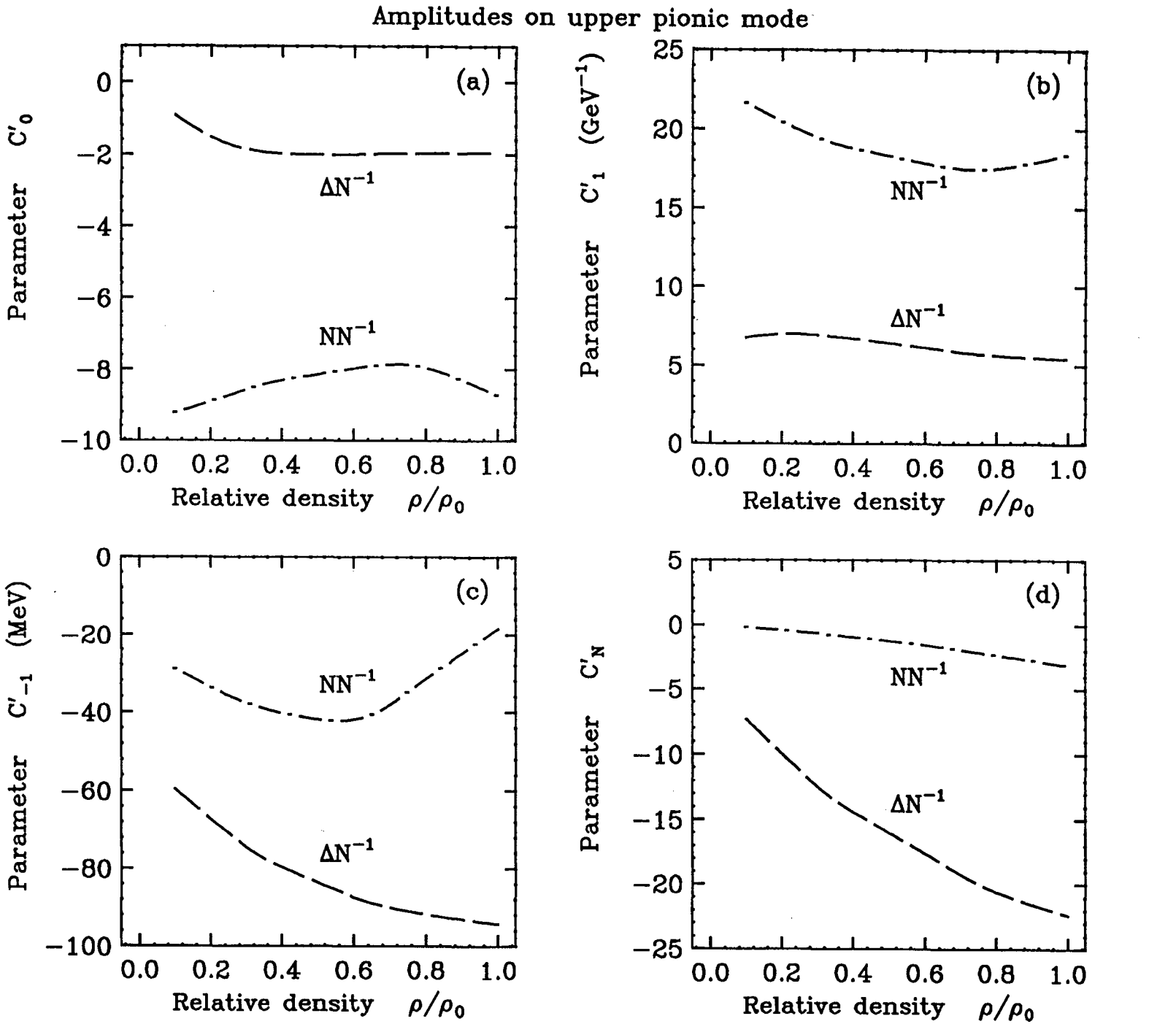
Amplitudes on upper pionic mode
(a)
Parameter C'_0
ΔN^{-1}
NN^{-1}
Relative density ρ/ρ_0
(b)
Parameter C'_1 (GeV^{-1})
NN^{-1}
ΔN^{-1}
Relative density ρ/ρ_0
(c)
Parameter C'_{-1} (MeV)
NN^{-1}
ΔN^{-1}
Relative density ρ/ρ_0
(d)
Parameter C'_N
NN^{-1}
ΔN^{-1}
Relative density ρ/ρ_0

FIGURE 6

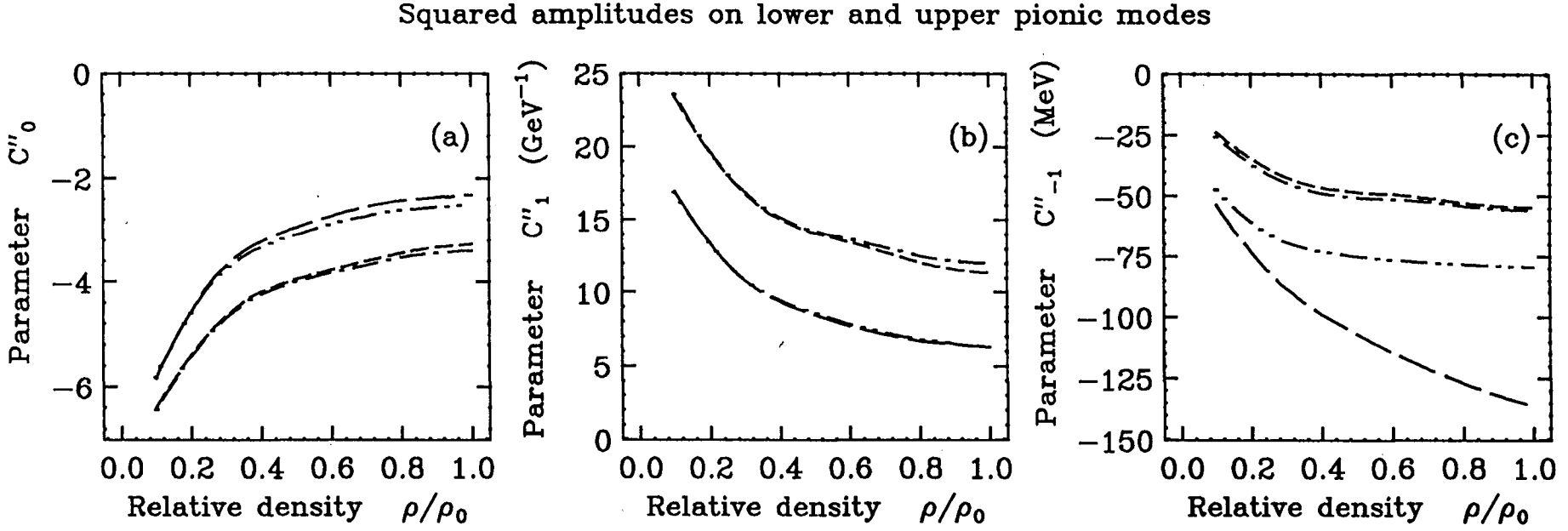
Squared amplitudes on lower and upper pionic modes
Parameter C''0
(a)
Relative density ρ/ρ0
Parameter C''1 (GeV−1)
(b)
Relative density ρ/ρ0
Parameter C''−1 (MeV)
(c)
Relative density ρ/ρ0

FIGURE 7

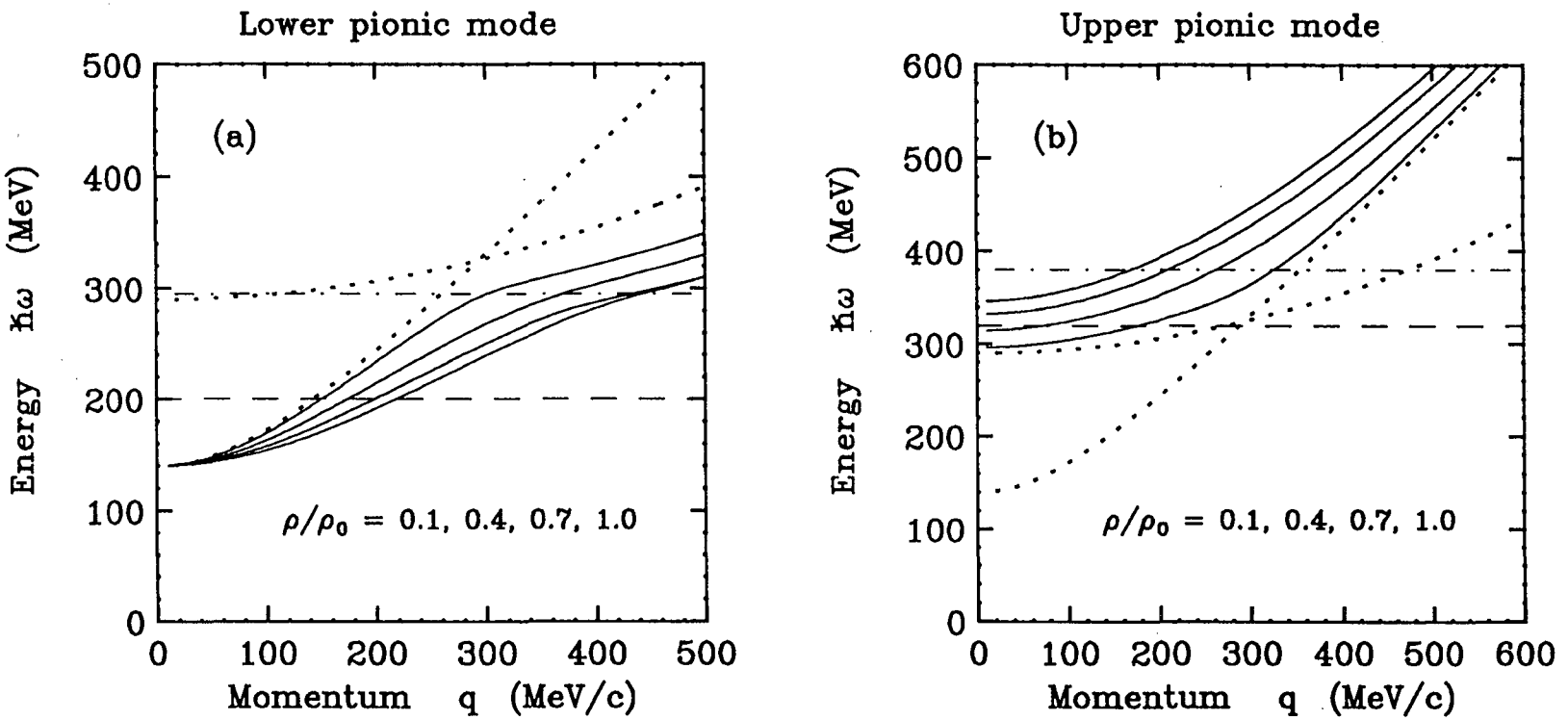
Lower pionic mode
(a)
Energy ħω (MeV)
Momentum q (MeV/c)
ρ/ρ0 = 0.1, 0.4, 0.7, 1.0
0
100
200
300
400
500
Upper pionic mode
(b)
Energy ħω (MeV)
Momentum q (MeV/c)
ρ/ρ0 = 0.1, 0.4, 0.7, 1.0
0
100
200
300
400
500
600

FIGURE 8

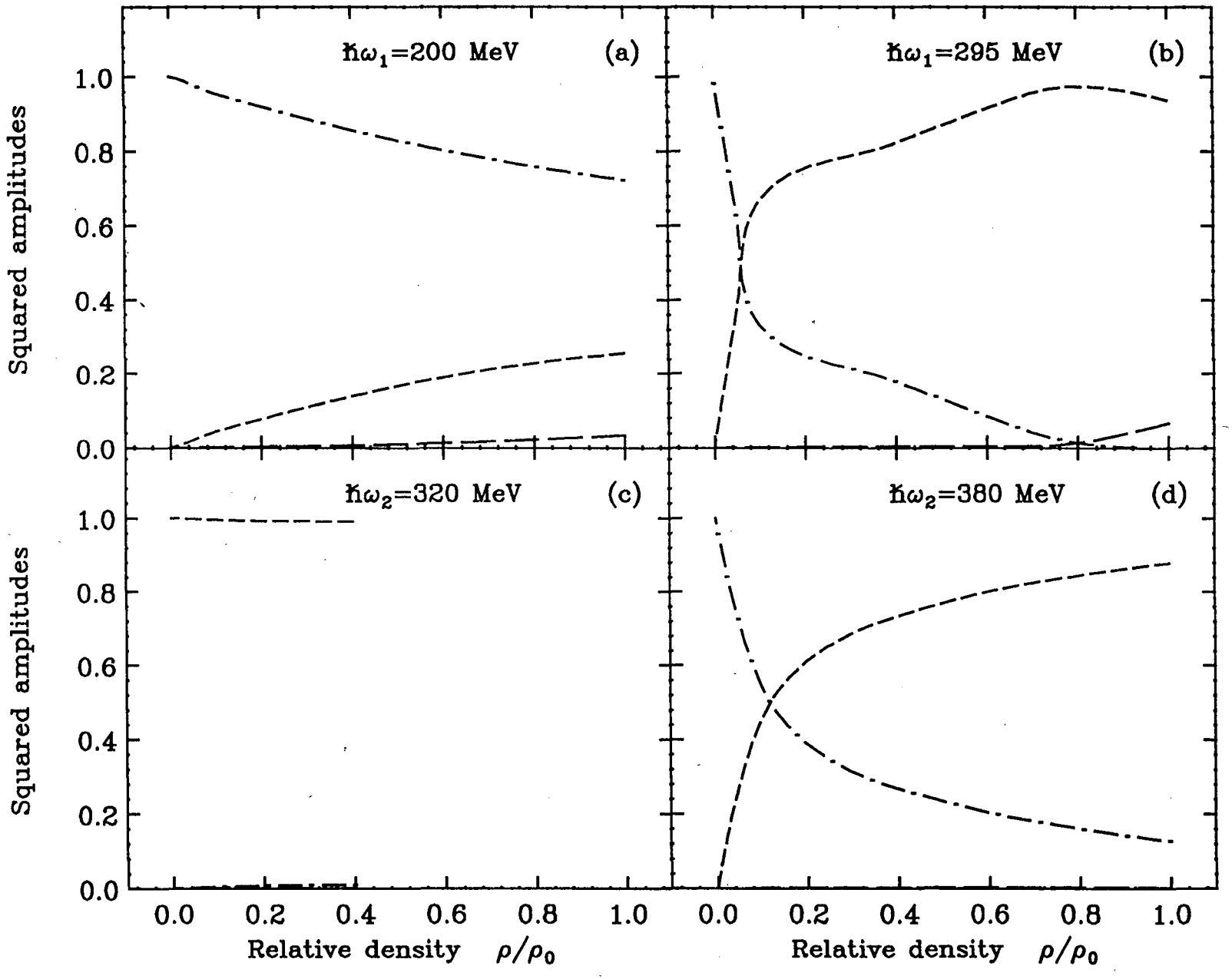
ħω1=200 MeV
(a)
ħω1=295 MeV
(b)
ħω2=320 MeV
(c)
ħω2=380 MeV
(d)
Squared amplitudes
Squared amplitudes
0.0
0.2
0.4
0.6
0.8
1.0
Relative density ρ/ρ0
Relative density ρ/ρ0

FIGURE 9

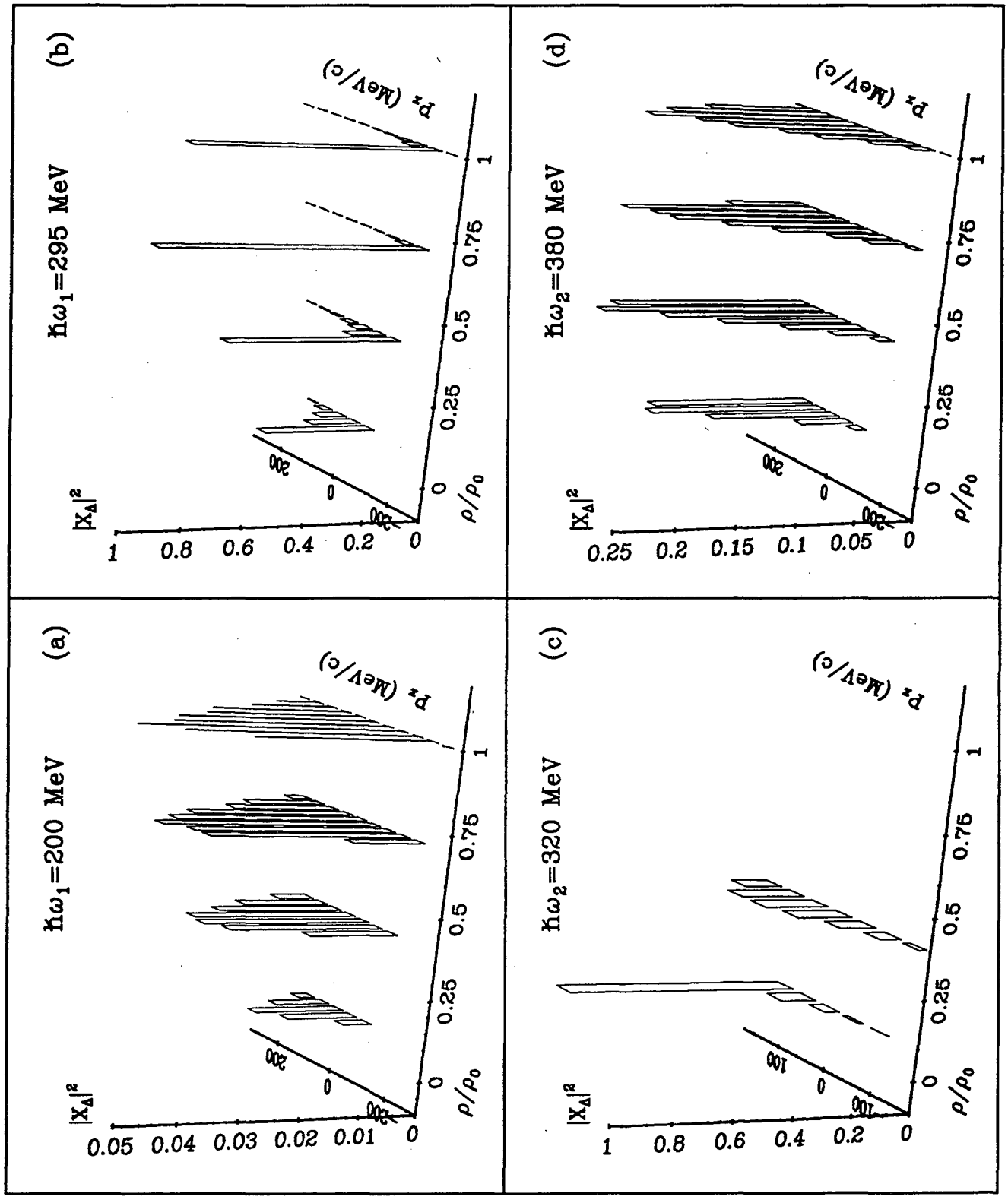
(a)
ħω1=200 MeV
(b)
ħω1=295 MeV
(c)
ħω2=320 MeV
(d)
ħω2=380 MeV
Pz (MeV/c)
ρ/ρ0
|χΔ|2

FIGURE 10

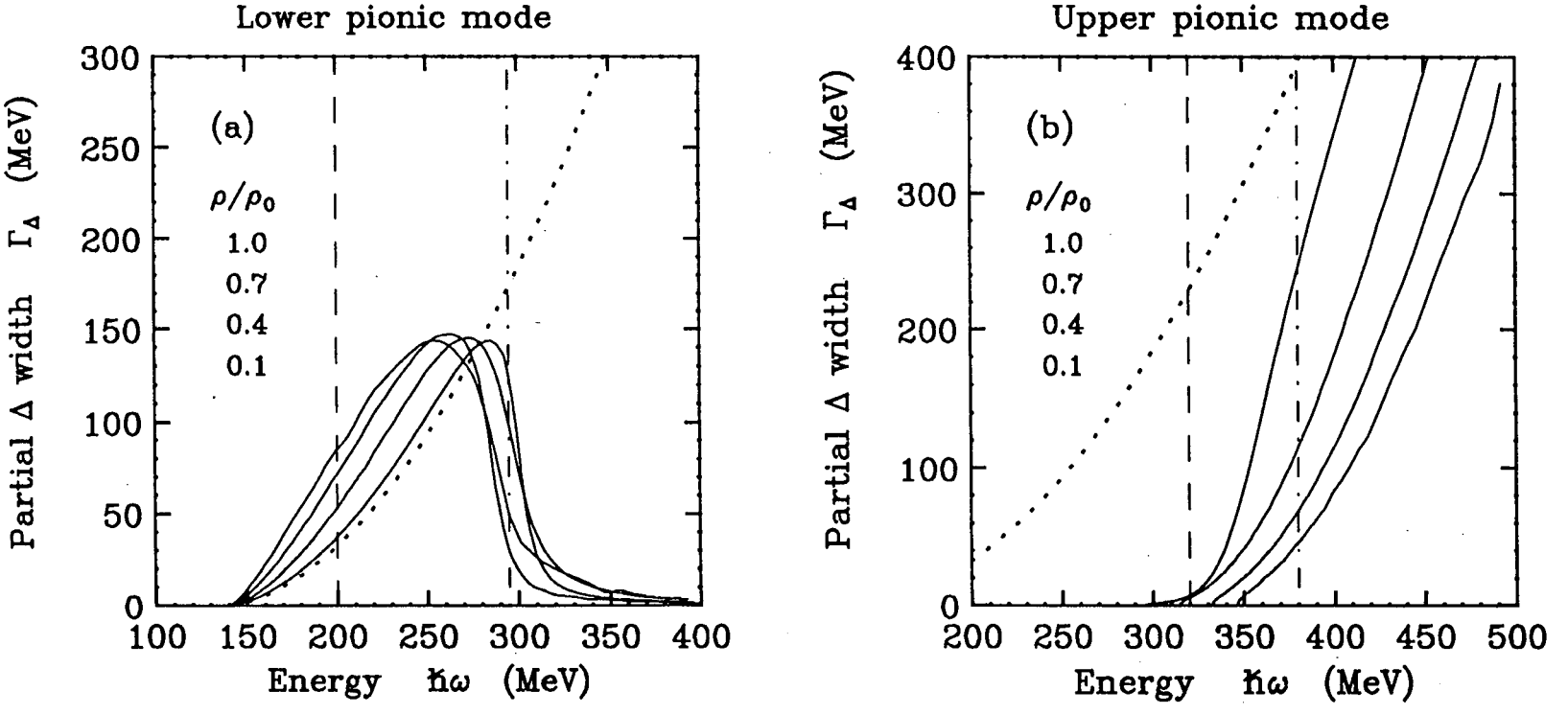
Lower pionic mode
Partial Δ width Γ_Δ (MeV)
(a)
ρ/ρ_0
1.0
0.7
0.4
0.1
Energy $\hbar\omega$ (MeV)
Upper pionic mode
Partial Δ width Γ_Δ (MeV)
(b)
ρ/ρ_0
1.0
0.7
0.4
0.1
Energy $\hbar\omega$ (MeV)

FIGURE 11

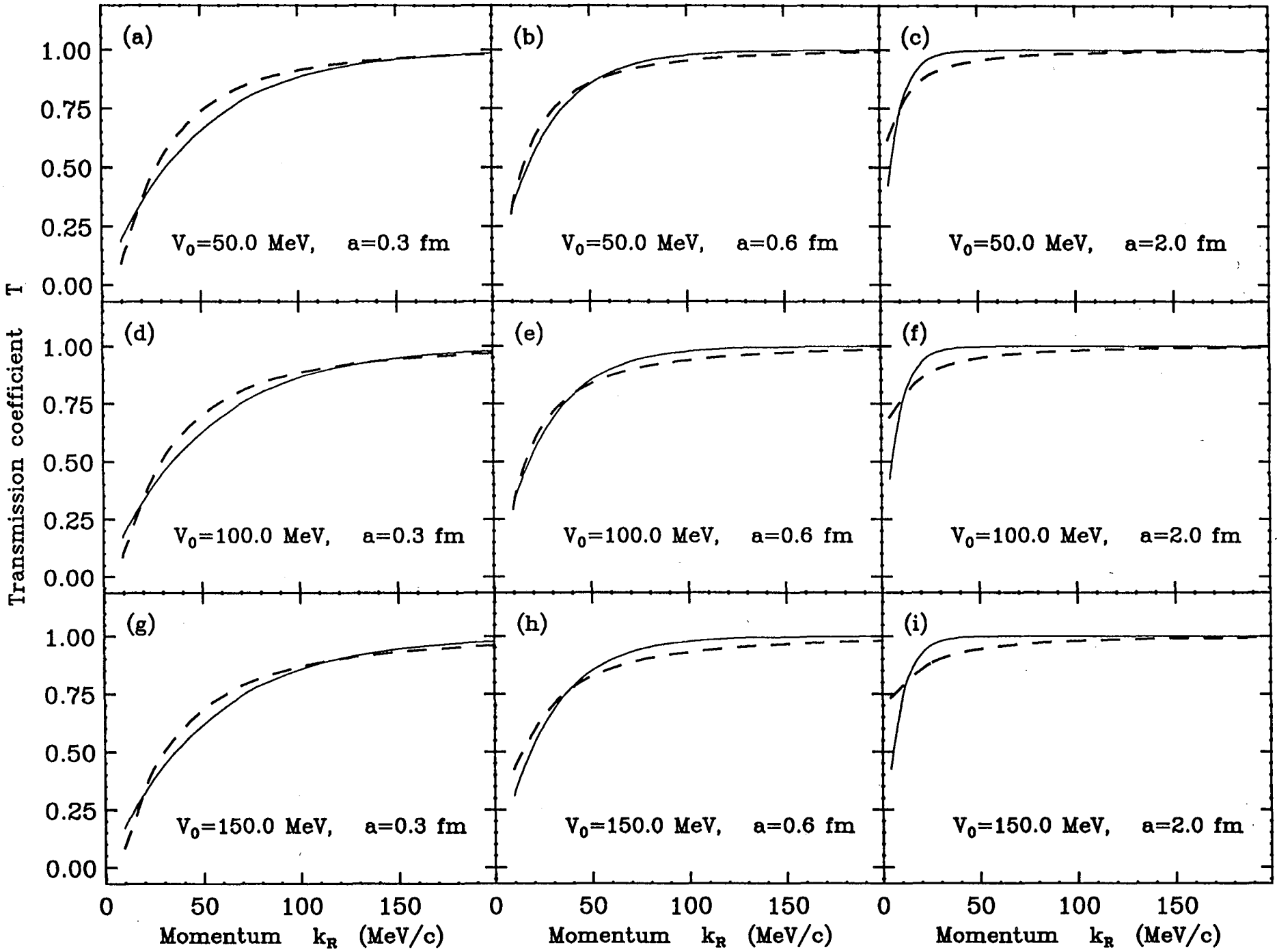
(a)
(b)
(c)
(d)
(e)
(f)
(g)
(h)
(i)
V_0=50.0 MeV, a=0.3 fm
V_0=50.0 MeV, a=0.6 fm
V_0=50.0 MeV, a=2.0 fm
V_0=100.0 MeV, a=0.3 fm
V_0=100.0 MeV, a=0.6 fm
V_0=100.0 MeV, a=2.0 fm
V_0=150.0 MeV, a=0.3 fm
V_0=150.0 MeV, a=0.6 fm
V_0=150.0 MeV, a=2.0 fm
Transmission coefficient T
0.00
0.25
0.50
0.75
1.00
0
50
100
150
Momentum k_R (MeV/c)

FIGURE 12

LAWRENCE BERKELEY LABORATORY
UNIVERSITY OF CALIFORNIA
TECHNICAL AND ELECTRONIC
INFORMATION DEPARTMENT
BERKELEY, CALIFORNIA 94720